1

Wing initial layout

2

THE WING IS KING

Wing initial layout — 1

THE WING IS KING

Wing layout has a number of determinants, and arguably it is the single most important aircraft component.

Once we know the weight of the aircraft, the two leading features to be chosen are wing loading W_0/S (i.e. the size of the the wing once we know W_0) and its shape, i.e. dimensionless numbers like aspect ratio A, taper ratio λ.

Other important features to be chosen are the airfoil section and high-lift system.

Two considerations that typically govern wing layout are (a) landing speed and (b) efficient cruise.

Ultimately the best choices for wing loading and layout will be established by constraint analysis and optimization. However at the initial stages of design layout, it is often useful to establish ball-park estimates so that the arrangement of the wing and fuselage can be fed into the design process.

Landing speed involves wing loading and high-lift system, while efficient cruise involves wing loading and the drag polar. Typically we will take the landing speed (or landing field length, which is closely related), as well as cruise altitude and speed, to be given in the design specification, although ultimately they are all open to variation and optimization.

Consideration of loading and layout for cruise is heavily influenced by aircraft aerodynamics because all the parameters for cruise are related to the minimum-drag speed V^*, and hence the aerodynamic parameters $C_{D,0}$ and $K = 1/(\pi Ae)$. At this stage we use reasonable or typical values for these parameters for the class of aircraft under consideration, and ultimately we would have to check the values through aerodynamic analysis.

Likewise for landing the airfoil and high-lift system (and through these, $C_{L\max}$) has to be chosen (at this stage, at least) on the basis of what is typically appropriate for the aircraft class.

(Schaufele's)

Selected wing information

Aircraft Type and Mission	(W/S) ~ psf
Personal/Utility Aircraft	10-30
Commuters - short range	30-50
Regional Turboprop Transports - short range	40-90
Business Jets - short to medium range	45-95
Jet Transports - short to medium range	80-120
Jet Transports - long range	120-160
Military Fighter Aircraft	60-110
Military Attack Aircraft	95-115

Fig. 4-1 Takeoff Wing Load Trends

$$C_L = \frac{W/S}{\frac{1}{2}\rho V^2} = \frac{W/S}{\frac{1}{2}\gamma p M^2}$$

$$(C_L/C_D)^* = \sqrt{\frac{\pi Ae}{4C_{D,0}}}$$

$$(C_L)^* = \sqrt{C_{D,0}\pi Ae}$$

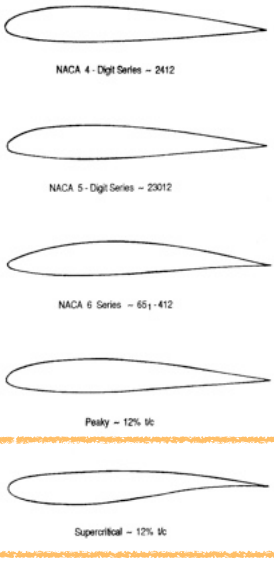

Business Jets	
Learjet 35	13.0
Gulfstream GIII	15.6
Single Aisle Twinjet Transports	
McDonnell Douglas MD-80	15.6
Boeing 737-300	15.1
Airbus A320	17.6
Boeing 757-200	17.1
Single Aisle Trijet Transport	
Boeing 727-200	16.2
Single Aisle Four Engine Jet Transport	
Boeing 707-320	18.6
Twin Aisle Twinjet Transports	
Airbus A300 B4	15.0
Boeing 767-200	18.1
Twin Aisle Trijet Transports	
Lockheed L1011-100	16.0
McDonnell Douglas DC-10-30	17.2
McDonnell Douglas MD-11	18.2
Twin Aisle Four Engine Jet Transport	
Boeing 747-400	17.4

Fig. 3-8 Cruise $(L/D)_{max}$ Values for Representative Civil Jet Powered Aircraft

AIRCRAFT TYPE	$C_{L_{MAX}}$ Clean	$C_{L_{MAX}}$ Takeoff	$C_{L_{MAX}}$ Landing
Personal/Utility	1.3-1.8	1.3-1.8	1.6-2.3
Commuters	1.3-1.8	1.4-2.0	1.6-2.5
Regional Turboprops	1.5-1.8	1.7-2.2	1.9-2.7
Business Jets	1.4-1.8	1.6-2.2	1.8-2.6
Jet Transports	1.4-1.8	1.6-2.2	1.8-3.0
Military Fighter/Attack	1.2-1.8	1.4-2.0	1.6-2.4

Fig. 4-4 Maximum Lift Coefficient Trends

Aircraft type	Aspect Ratio	Taper Ratio
Personal/Utility	5.0 - 8.0	1.0 - 0.6
Commuters	9.0 - 12.0	1.0 - 0.5
Regional Turboprops	11.0 - 12.8	0.6 - 0.4
Business Jets	5.0 - 8.8	0.6 - 0.4
Jet Transports	7.0 - 9.5	0.4 - 0.2
Military Fighter/Attack	2.4 - 5.0	0.5 - 0.2

Fig. 4-9 Wing Aspect Ratio and Taper Ratio Trends

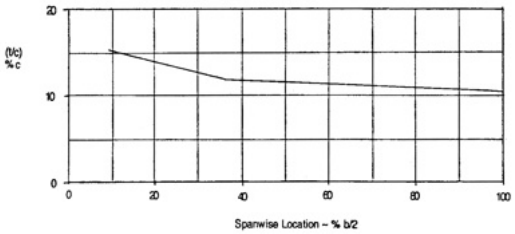

Fig. 4-10 Typical Wing Thickness Distribution for a Jet Transport

Wing initial layout — 2

We will use an example of the initial, approximate, wing layout process from Schaufele's book.

NB: wing loading values assume energy density of hydrocarbon fuel.

The first consideration is an appropriate range of take-off wing loadings W_0/S. At this stage we use information for comparable aircraft in the class as a basis for comparison.

Aircraft Type and Mission	(W/S) ~ psf	Pa
Personal/Utility Aircraft	10-30	500–1500
Commuters - short range	30-50	1400–2400
Regional Turboprop Transports - short range	40-90	1900–4300
Business Jets - short to medium range	45-95	2200–4500
Jet Transports - short to medium range	80-120	3800–5800
Jet Transports - long range	120-160	5800–7700
Military Fighter Aircraft	60-110	2900–5300
Military Attack Aircraft	95-115	4500–5500

1. Plot a graph with W_0 and S as axes, with limit lines for the appropriate class wing loading trend data.

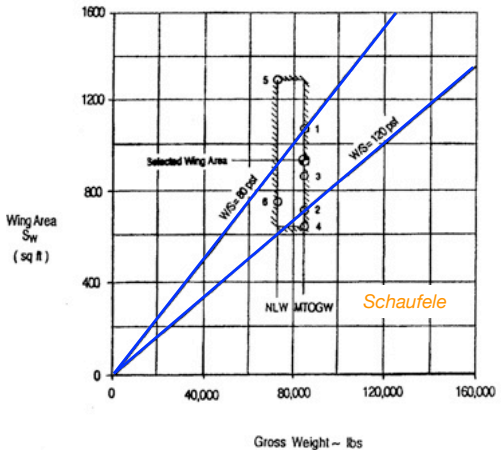

Related Data	
Cruise Mach number	0.76
Cruise Altitude	31,000 ft
MTOGW	85,000 lb
OEW	50,000 lb
Payload (80 pass)	16,400 lb
Reserve Fuel	5,800 lb
NLW	72,200 lb
V_{APP}	125 kts
q @ V_{APP}	53.2 psf
q @ ICA	243.2 psf

Here the limit lines are for a short-range jet transport.

W_0/S = 80 – 120 lbf/ft^2.

Wing initial layout — 3

2. At MTOW (here called MTOGW) identify the two corresponding wing areas S_1 and S_2 on the limit lines.

$$S = \frac{W_0}{W/S} \qquad S_1 = \frac{85,000}{80}\,\text{ft}^2 = 1062.5\,\text{ft}^2$$

$$S_2 = \frac{85,000}{120}\,\text{ft}^2 = 708.3\,\text{ft}^2$$

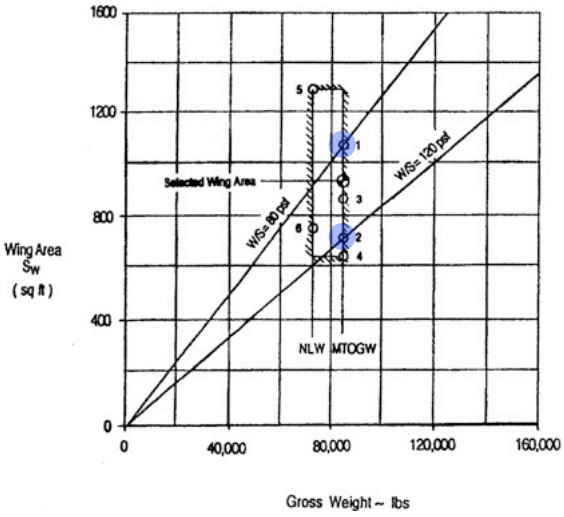

3. Find the wing area(s) required to meet the initial cruise altitude and speed specified at an appropriate C_L. ($C_{L,\text{des}}$)

Function	*Dimensionless*	*V/V*, at max*	*(L/D)/(L/D)*, at max*	*C_L/C_L*, at max*
$L(DV)$	$C_L^{3/2}/C_D$	$(1/3)^{1/4} = 0.760$	$(3/4)^{1/2} = 0.866$	$3^{1/2} = 1.732$
L/D	C_L/C_D	1	1	1
$(VL)/D$	$C_L^{1/2}/C_D$	$(3)^{1/4} = 1.316$	$(3/4)^{1/2} = 0.866$	$(1/3)^{1/2} = 0.577$

Choosing an appropriate $C_{L,\text{des}}$ requires some thought because it depends on

a. the propulsion class, and so how $C_{L,\text{des}}$ relates to C_L* (value at $L/D_{\max}$) in the main flight task (range or endurance) as per the above table;

b. aerodynamics, through $C_{D,0}$ and K, since $C_L^* = (C_{D,0}/K)^{1/2}$, and we may find $C_{D,0}$ and K need some analysis to establish in advance (and note that we can manipulate K, at least, via wing aspect ratio);

c. transonic drag rise, if present. Subsonic jet transport aircraft typically are designed to cruise at M_{DD}, the drag-divergence Mach number, in which case it is typical to cruise at a C_L closer to C_L* than $0.577C_L$*, as the above table would suggest is appropriate for (jet) cruise range maximization.

At this stage however, where we are just seeking to establish a reasonable value of S, it is acceptable to use typical historical data for C_L*, and choose $C_{L,\text{des}}$ appropriately in relation to it.

Wing initial layout — 4

Aircraft category	*Typical range of C_L**
personal/utility, commuters, regional turboprops	0.60 – 0.75
business, commercial, military transport jets	0.40 – 0.55
military fighter/attack, high subsonic cruise	0.32 – 0.40
supersonic transports/bombers	0.12 – 0.15

Note that we previously gave related information under the heading Typical aerodynamic parameters.

For transonic jet transports, as stated above we typically find the range cruise condition is flown where the requested cruise speed can be assumed equivalent to M_{DD}, and the maximum range parameter is achieved near $M_{DD}(L/D)^*$, with $C_{L,\text{des}} = C_L$*.

At the specified cruise height (31,000 ft) and Mach number (0.76), the dynamic pressure q = 242.8 lbf/ft².

To be a little conservative (it is better to err on the side of a lower than a higher wing loading), the related S values are typically computed for MTOW W_0 at the limits of the $C_{L,\text{des}}$ range.

$$S = \frac{W_0}{C_{L,\text{des}}\,q} \qquad S_3 = \frac{85,000}{0.40 \times 242.8}\,\text{ft}^2 = 875.2\,\text{ft}^2$$

$$S_4 = \frac{85,000}{0.55 \times 242.8}\,\text{ft}^2 = 636.5\,\text{ft}^2$$

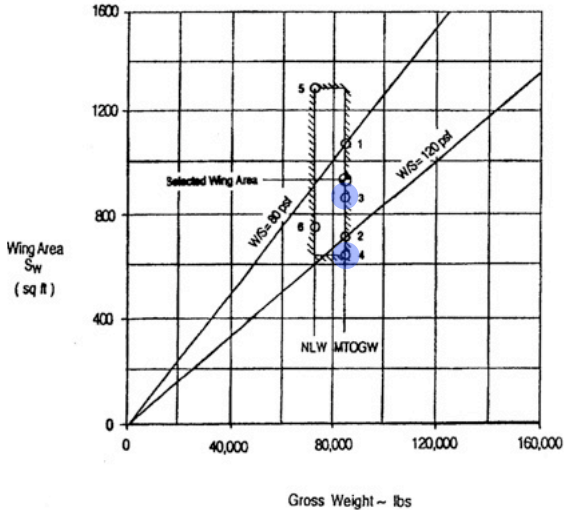

Wing initial layout — 5

4. Find the wing areas required to meet landing approach speed requirement (here it was V_{app} = 125kt) at NLW (here 72,200 lbf) and considering the likely range of maximum lift coefficient that the high-lift system for this type of aircraft might deliver in landing configuration.

Aircraft Type	Speed (kts)
Personal/Utility Aircraft	75
Turboprop Commuters	105
Regional Turboprops	110
Business Jets	120
Short Range Jet Transports	125
Long Range Jet Transports	150
Military Fighter/Attack Aircraft	150

Fig. 4-3 Maximum Landing Approach Speeds

AIRCRAFT TYPE	$C_{L_{MAX}}$ Clean	$C_{L_{MAX}}$ Takeoff	$C_{L_{MAX}}$ Landing
Personal/Utility	1.3-1.8	1.3-1.8	1.6-2.3
Commuters	1.3-1.8	1.4-2.0	1.6-2.5
Regional Turboprops	1.5-1.8	1.7-2.2	1.9-2.7
Business Jets	1.4-1.8	1.6-2.2	1.8-2.6
Jet Transports	1.4-1.8	1.6-2.2	1.8-3.0
Military Fighter/Attack	1.2-1.8	1.4-2.0	1.6-2.4

Fig. 4-4 Maximum Lift Coefficient Trends

Landing approach speed V_{app} is typically required to be at least $1.3V_{stall}$.

This makes the approach $C_{Lapp} = C_{Lstall} / 1.3^2 = C_{Lstall} / 1.69$.

The dynamic pressure at V_{app} is q = 53.2 lbf/ft².

$$S = \frac{W_{NLW}}{C_{L,app} q_{app}} \qquad S_5 = \frac{72,200}{(1.8/1.69) \times 53.2}\,\text{ft}^2 = 1274.2\,\text{ft}^2$$

$$S_6 = \frac{72,200}{(3.0/1.69) \times 53.2}\,\text{ft}^2 = 764.5\,\text{ft}^2$$

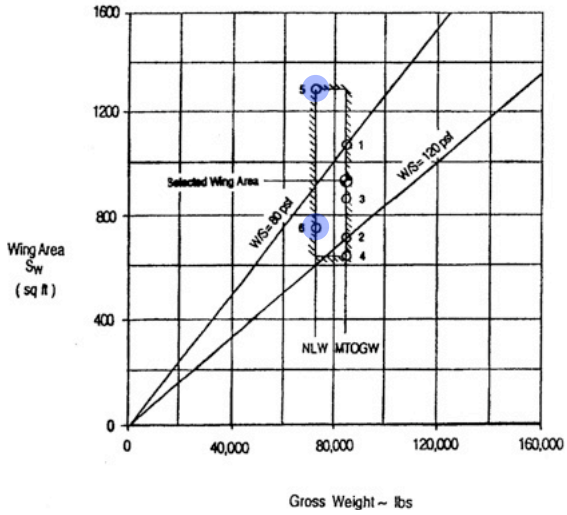

Wing initial layout — 6

5. Now we have three wing area ranges and it's a matter of choosing an appropriate value to work with.

Historical data: $S_{1,2}$ = 708 – 1062 ft²

Initial cruise: $S_{3,4}$ = 635 – 874 ft²

Landing approach speed: $S_{5,6}$ = 764 – 1274 ft²

A reasonable value that meets all the requirements is S = 850 ft².

Note that it is generally better to have a wing area that is on the larger end of the requirement band since

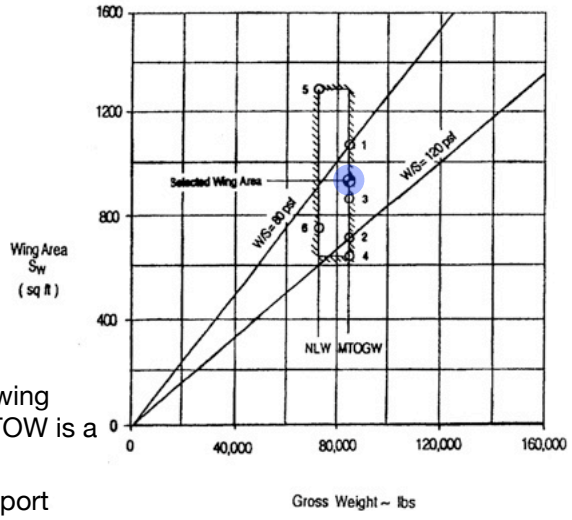

a. MTOW W_0 tends to increase as the design matures. A wing area that cannot accommodate modest increases in MTOW is a severe restriction.

b. Historical evidence suggests that especially for jet transport aircraft, later versions are typically 'stretched' in the fuselage to accommodate more passengers. Simple enough to do this to the fuselage (basically a big tube: add inserts), but costly to change the wing.

Hence in this case it was judged reasonable to increase the initial design wing area by a further 10%, so that $S = 1.1 \times 850$ ft² = 935 ft².

Note that this implies we may need to alter our initial cruise altitude to recover most efficient cruise, at least for the early design variants.

If we find we cannot get the required wing areas for the different requirements to be even close to overlapping, we may have to consider other design options (e.g. power-assisted high-lift systems).

A note on ‘Drag Divergence’ Mach number

C_D increases rapidly with Mach number in the transonic regime, as shock systems start.

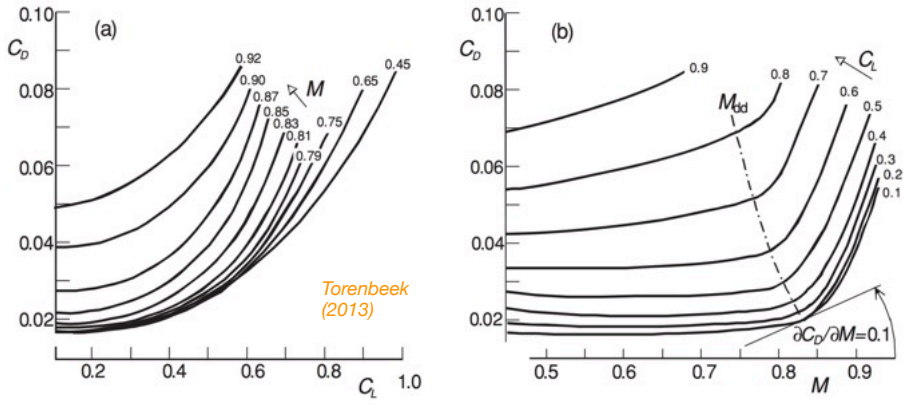

Figure 4.11 Drag coefficients of a transonic airliner. (a) C_D versus C_L for different Mach numbers. (b) C_D versus M for different lift coefficients

The associated Mach number is called the ‘drag divergence‘ value, typically abbreviated as M_{DIV} or M_{DD}.

M_{DD} usually falls with increasing C_L since the shock systems involved usually begin on the wing suction surface.

Two alternative definitions (typically the values are quite close):

1. M_{DD} occurs when C_D rises 20 ‘drag counts’ above the $M \rightarrow 0$ value. One ‘drag count’ is 0.001, so this is a rise of 0.02.
2. M_{DD} occurs when $\partial C_D/\partial M$=0.1.

The best value for jet aircraft range parameter ML/D usually occurs near M_{DD}: if the stated cruise M is ‘obviously’ transonic, assume it is very close to M_{DD}, and design accordingly.

Wing airfoil selection

1. Selection is primarily dependent on the flight speed regime.
2. Symmetrical NACA 4-digit series airfoils (e.g NACA 0009) are still often used for empennage (‘tailfeathers’).
3. For subsonic personal/utility, commuter and regional turboprop, NACA 5-digit series are good since they have a high maximum lift and good thickness. NASA GA/LS series is also good, or better.
4. For high-subsonic business jets, commercial jet transports and military cargo jets, ‘modern’ supercritical airfoils are first choice owing to higher values of M_{DD}. Other desirable features may be somewhat compromised.
5. For supersonic military fighter/attack aircraft, usual choice is a thin (<5%) NACA 6-series airfoil for reasonable characteristics at both subsonic and supersonic speeds.
6. For supersonic transports (rare!) the whole wing is a complex integrated surface, optimized by computer and so ‘airfoil selection’ does not have much significance.
7. For high-performance applications or where fuel economy is critically important, sections are now typically optimized using a computer for the specific application, starting from one of the above choices.
8. The airfoil section is very often varied along the span for both aerodynamic and structural reasons.

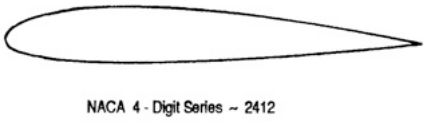

NACA 4 - Digit Series ~ 2412

NACA 5 - Digit Series ~ 23012

NACA 6 Series ~ 65_1 - 412

Peaky ~ 12% t/c

Schaufele

Supercritical ~ 12% t/c

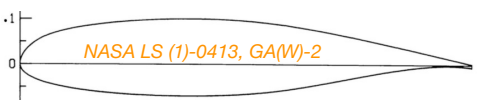

NACA airfoil nomenclature FYI

NACA/NASA airfoils are widely used and well documented, e.g. in Abbott & Doenhoff, NACA TR 824.

1. NACA 4-digit series:

$$\pm y_t = \frac{t}{0.20}\left(0.29690\sqrt{x} - 0.12600x - 0.35160x^2 + 0.28430x^3 - 0.10150x^4\right)$$

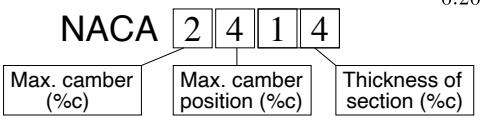

Historically the first, no longer much used as wing airfoils, but symmetrical variants common for tail surfaces.

2. NACA 5-digit series:

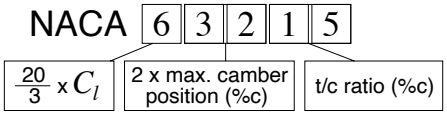

Designed to achieve higher C_{lmax} than the 4-digit series (uses same thickness distribution). Note the indication of a target C_l value.

3. NACA 6-series (confusingly, the third digit can be a subscript, and sometimes omitted!):

See Abbott & von Doenhoff for the full nomenclature.

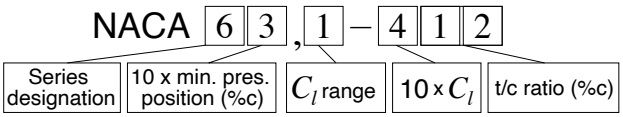

Originally designed to achieve laminar flow over a substantial fraction of the chord (hence reduce drag). In fact the surface must be kept very smooth and clean to achieve this. Performance is still good even if laminar flow cannot be preserved, but C_{lmax} values may be lower than equivalent 5-digit airfoil. Note the indication of a target C_l value.

Wing thickness, aspect and taper ratios

Choice of wing thickness ratio *t/c* comes about as a balance between structural, aerodynamic and volume considerations.

The *t/c* ratio is maximum around 15% for subsonic aircraft and falls as design maximum speed rises.

Aircraft category	*Typical $(t/c)_{avg}$*
personal/utility, commuters, regional turboprops	0.12 – 0.15
business, commercial, military transport jets	0.09 – 0.12
supersonic-capable	0.03 – 0.05

The airfoil section (and *t/c* ratio) can vary along the span. If the wing is approximated as a trapezoidal planform shape, an appropriate average thickness can be computed.
Here *R* is for root and *T* for tip values.

$$(t/c)_{\text{avg}} = \frac{t_R + t_T}{c_R + c_T}$$

Choice of wing aspect ratio *A* comes about as a balance between the aims of achieving an appropriate ratio of C_L/C_D (i.e. the relationship between $C_{D,0}$ and *K*) at cruise, and of keeping wing weight, which increases with aspect ratio, low.

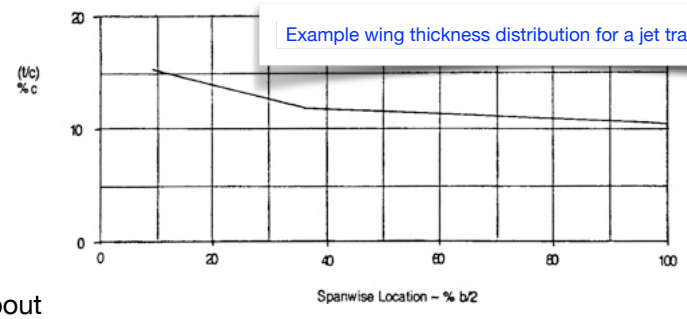

Example wing thickness distribution for a jet transport aircraft.

Schaufele

Choice of wing taper ratio λ comes about as a balance between requirements for efficient span load distribution at cruise, stall characteristics, and wing strength.

Typical values of aspect and taper ratios for different aircraft categories are shown.

	$A = b^2/S$	$\lambda = c_t/c_0$
Aircraft type	Aspect Ratio	Taper Ratio
Personal/Utility	5.0 - 8.0	1.0 - 0.6
Commuters	9.0 - 12.0	1.0 - 0.5
Regional Turboprops	11.0 - 12.8	0.6 - 0.4
Business Jets	5.0 - 8.8	0.6 - 0.4
Jet Transports	7.0 - 9.5	0.4 - 0.2
Military Fighter/Attack	2.4 - 5.0	0.5 - 0.2

Wing sweepback angle

The central principle of using wing sweep for transonic aircraft in particular is based on recognition that only the component of velocity normal to the wing produces lift and hence results in flow speed-up and onset of compressibility-related drag. Thus the onset of these effects with freestream Mach number can be delayed by introducing wing sweep (angle Λ).

$$V_{\text{eff}} = V_\infty \cos\Lambda$$
$$M_{\text{eff}} = M_\infty \cos\Lambda$$
$$q_{\text{eff}} = q_\infty \cos^2\Lambda$$

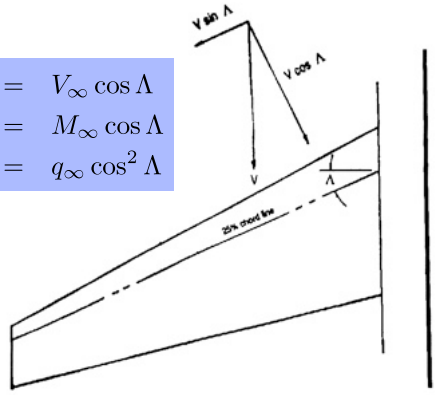

For transonic aircraft the sweep angle Λ is taken at the $c/4$ line for the wing.

For subsonic aircraft wing sweep is generally of no benefit, while for genuinely supersonic aircraft, selection of sweep angle is more complex than we can address here.

The *crest-critical* Mach number M_{CC} (freestream M_∞ where the local Mach number at the airfoil minimum-C_p location first reaches $M = 1$), and through this the *drag-divergence* Mach number M_{DD} depend on (a) airfoil section and its t/c ratio (b) cruise design $C_{L\text{des}}$ and wing sweep angle Λ.

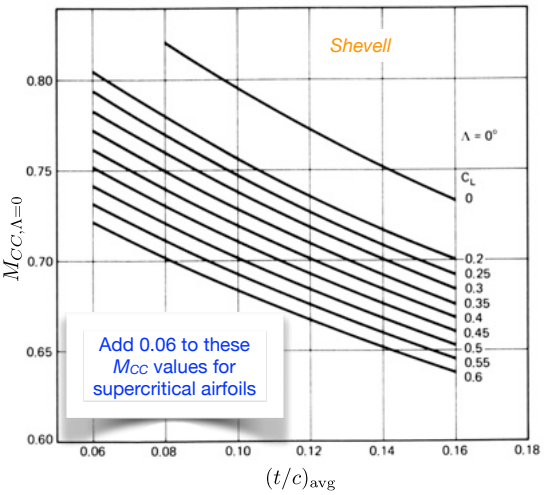

The design task typically starts with M_{DD}, $C_{L\text{des}}$ and $(t/c)_{\text{avg}}$, and requires Λ to be found.

One method involves inverting this set of relationships from Shevell:

$$M_{DD} = M_{CC}[1.02 + 0.08(1 - \cos\Lambda)]$$

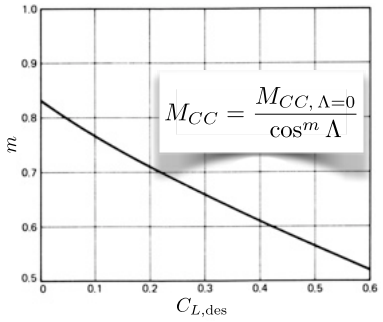

Wing sweepback angle

An apparently different method is presented by Schaufele (but in fact it is based largely on the same information as Shevell's). It involves interpolating in wing design charts to establish one of the four variables Λ, $C_{L\text{des}}$, $(t/c)_{\text{avg}}$ and M_{DD}, given the other three.

Remaining things to be established for the initial wing layout are

1. Type and spanwise extent of the high-lift system;
2. Type and spanwise extent of lateral control devices (ailerons and spoilers);
3. Wing mean aerodynamic chord;
4. Estimation of wing spar locations and available wing fuel volume;
5. Wing inboard trailing edge extensions to house landing gear within swept wings.

We have previously dealt with layout or determination of all of the above with the exception of (5), which we will deal with in discussing landing gear design.

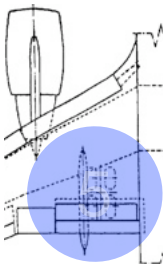

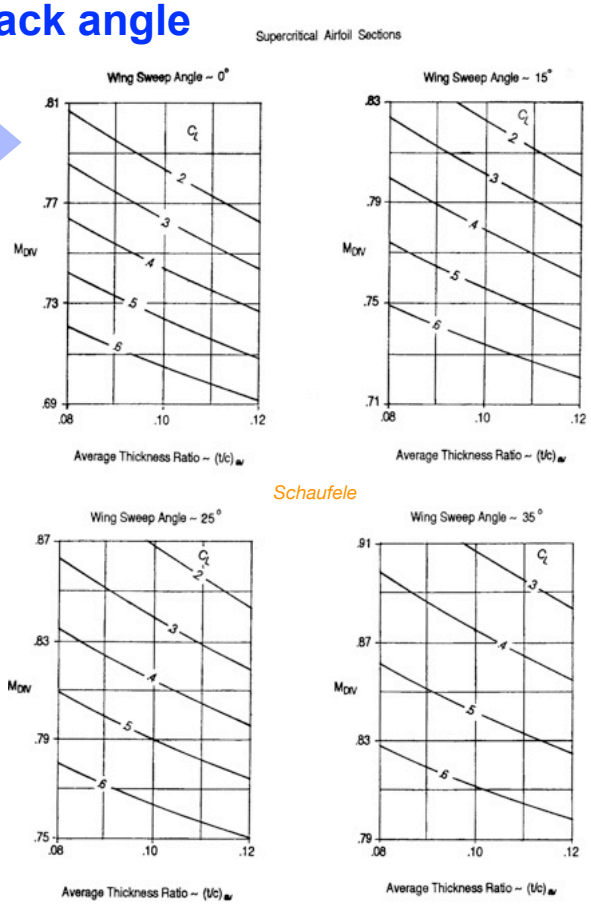

Fig. 4-8 Wing Design Charts for Transonic Cruise Aircraft

Wing layout line diagram

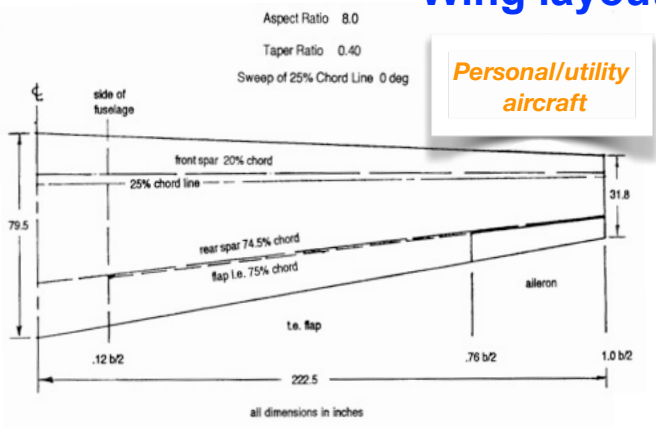

Personal/utility aircraft

To firm up wing layout issues, it is recommended to produce a wing layout line diagram and check that proportions and relative locations are reasonable before proceeding to 3-view drawing stage.

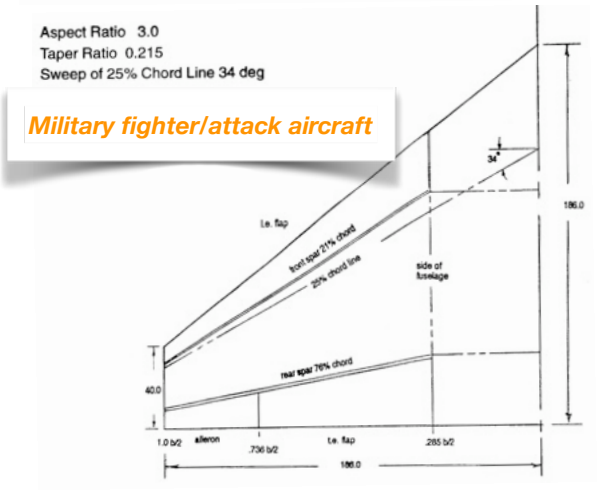

Military fighter/attack aircraft

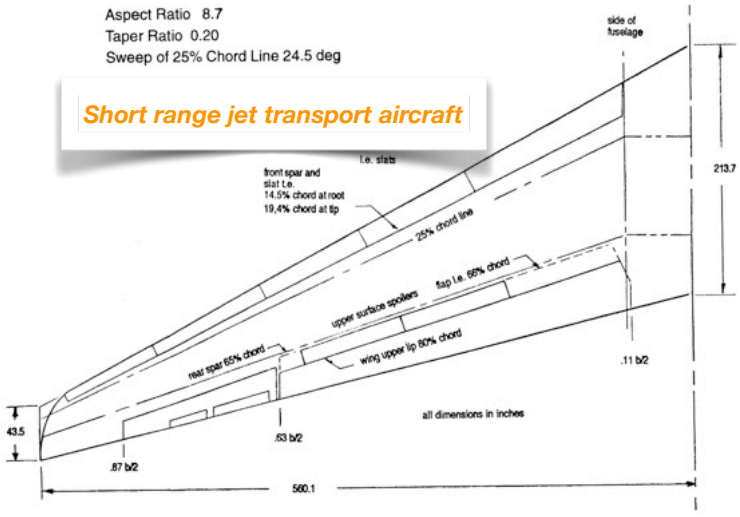

Short range jet transport aircraft

Schaufele

Practical aerodynamics

Airfoil nomenclature and performance — 1

1. An airfoil is a 2D slice of a 3D wing.
2. The angle of attack (AOA) α is the angle made between the airfoil's chord line (drawn between the frontmost and rearmost locations on the airfoil, the LE and TE) and the oncoming flow vector ***V***. Length of chord line is conventionally labelled *c*.
3. Flow past an airfoil causes a force per unit length normal to the page *R'* plus a moment per unit length, *M'*.
4. Conventionally the force is resolved into lift (per unit length) *L'* and drag (per unit length) *D'*, normal and parallel to the oncoming flow ***V***. The magnitude of ***V*** is *V* or V_∞.
5. The value of moment *M',* depends on the axis about which moments are taken, but *M'* is approximately independent of α if when the point is c/4 behind the L.E. (This is an exact theoretical location for inviscid flow past thin airfoils.) For initial design purposes this *c*/4 location is taken as the airfoil's aerodynamic centre about which moments are considered.
6. By convention a positive moment *M'* causes a nose-up pitch, however conventional airfoils with positive camber create a negative/nose-down pitching moment about the *c*/4 location.
7. In general, *L', D'* and *M'* are functions of AOA α, Reynolds number *Re*=*Vc*/ν, and Mach number *M*=*V*/*a*.
8. We define dimensionless coefficients of lift, drag, and moment by dividing by dynamic pressure and chord (or chord²). They are denoted as sectional (2D) values by lowercase subscripts.

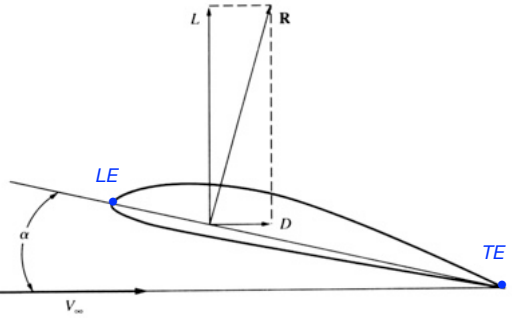

Anderson

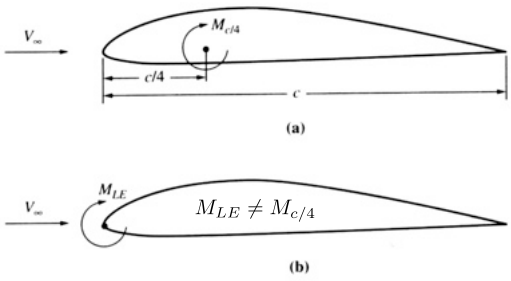

$$C_l = \frac{L'}{\frac{1}{2}\rho V^2 c} = f_1(\alpha, Re, M)$$

$$C_d = \frac{D'}{\frac{1}{2}\rho V^2 c} = f_2(\alpha, Re, M)$$

$$C_{m_{c/4}} = \frac{M'_{c/4}}{\frac{1}{2}\rho V^2 c^2} = f_3(\alpha, Re, M)$$

Airfoil nomenclature and performance — 2

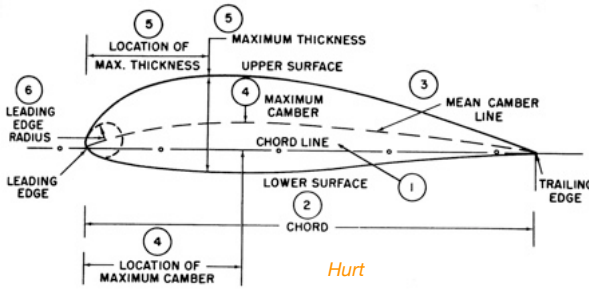

Hurt

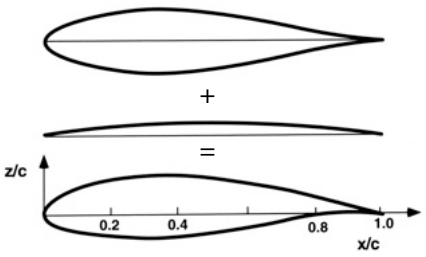

Thomas

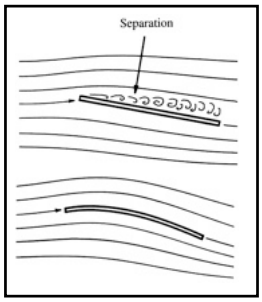

Raymer

9. Any airfoil profile can be decomposed into the sum of a thickness distribution and a (mean) camber line.
10. Thickness and camber can be changed independently and have largely independent effects on airfoil performance, at least for non-transonic flows. For transonic flows (*M*≈1), the two sides of the airfoil are typically shaped quasi-independently without using the decomposition.
11. **We typically want the maximum possible profile thickness to gain structural strength and internal volume (for fuel, landing gear stowage).** Up to a point, increasing thickness and nose radius increase the maximum lift coefficient, but since they also increase peak suction they also lower the Mach number for onset of wave drag, which will be important if the aircraft is designed for transonic cruise. For aircraft with supersonic wings, thickness must be kept small (e.g. <5%).
12. The thickness distribution can be chosen to change the boundary layer characteristics and move the location of BL turbulent transition (typically, as far downstream as possible, to reduce drag).
13. **The camber distribution is typically used to shift α for minimum C_d close to that for the design C_l.**
14. However, the camber distribution can also be used to influence the pitching moment, $C_{m,c/4}$. If we need to influence both C_d vs C_l and $C_{m,c/4}$, something else will be compromised, typically $C_{l\max}$.

Airfoil nomenclature and performance — 3

Generic lift, drag, moment curves for a symmetrical airfoil.

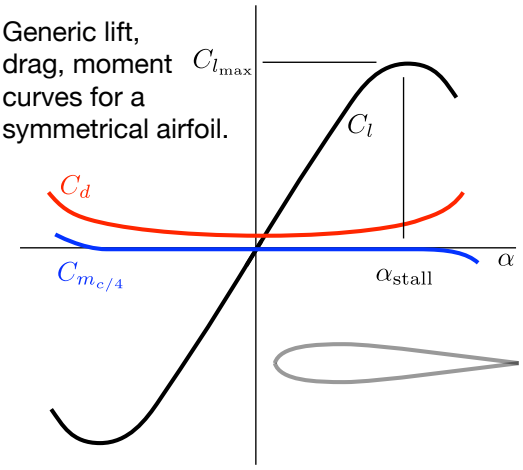

Generic lift, drag, moment curves for a cambered airfoil.

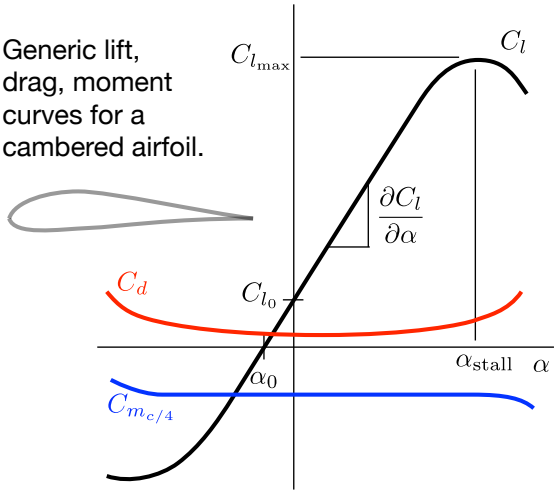

15. For a symmetrical airfoil, C_l is an odd function, C_d an even function of α and $C_{m,c/4}$=0 (away from stall).
16. In level unaccelerated flight, a positive value of L' or C_l is required to support aircraft weight.
17. The reason for adding camber is to place the minimum C_d (or maximum L/D) at the design value of C_l.
18. Adding camber moves the lift curve up and to the left. There is a positive value of C_l at α=0, and the maximum (stall) C_l is greater than for the equivalent symmetric airfoil. Also, $C_{m,c/4}$ becomes negative.
19. The theoretical lift curve slope for a thin airfoil is $\partial Cl/\partial\alpha=2\pi$, and this is always a good initial estimate.
20. Stall, associated with flow separation on the suction side of airfoil, is defined to occur at C_{lmax}. Typical values of C_{lmax} are in the range 1 to 2, stall angles of attack of order 12° to 20°.
21. For viscous/real flows, C_d is always positive (and small), initially increases approximately quadratically with C_l, then more rapidly at stall. This drag, related to the 2D airfoil profile, is called profile drag(!).

Airfoil nomenclature and performance — 4

An airfoil polar diagram shows the sectional lift and drag coefficients plotted against one another with the angle of attack α as a parameter.

'Polar diagram' is just the conventional name for a plot that shows a vector of total force and the two orthogonal components that make it up as a function of a parameter (α).

Up to the stall point, the sectional drag coefficient is approximately a quadratic function of lift coefficient.

$$C_d \approx C_{d_{\min}} + kC_l^2$$

Note that $C_l \gg C_d$.

Also that C_{dmin} is very small.

Soon, we will see lift/drag polar diagrams for the whole aircraft. Do not be confused — they are different diagrams, though with similar characteristics.

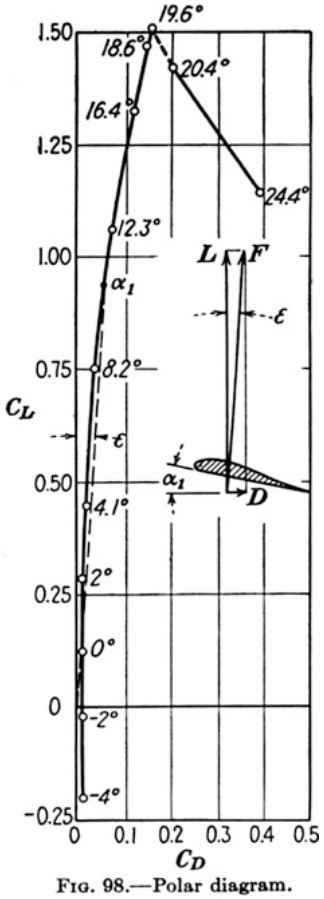

Fig. 98.—Polar diagram.

von Mises

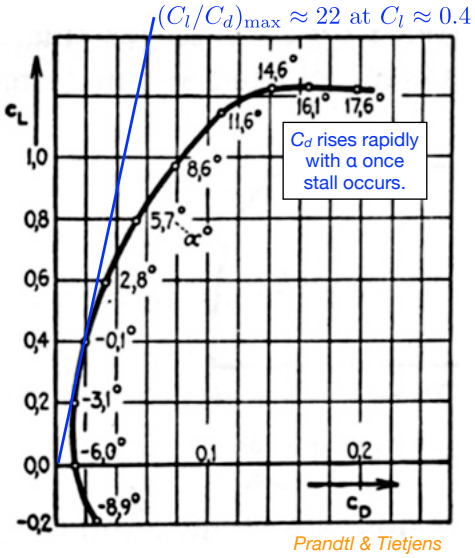

Prandtl & Tietjens

The value $(C_l/C_d)_{max}$ is the primary measure of airfoil efficiency, and the value of C_l for which this is achieved is a first approximation to the whole-aircraft value (at infinite aspect ratio) often used in initial design.

Typically in aircraft design, we work with C_l as a design variable and ignore α, except when required.

Airfoil nomenclature and performance — 5

Minimizing C_d at design C_l:

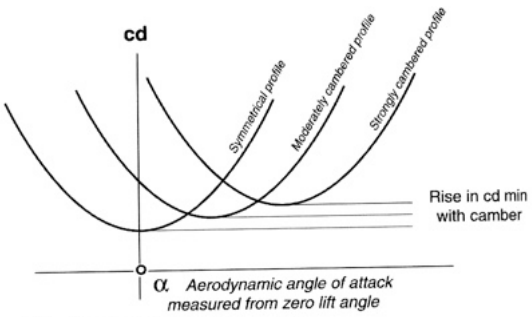

(A) Profile drag plotted against angle of attack

Simons

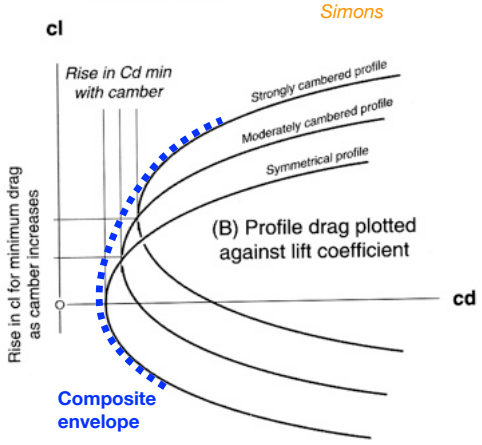

Drag polar

Effect on C_d of increasing camber:
1. α(C_{dmin}) increases;
2. C_{dmin} increases;
3. **Drag polar moves up and right**.
   (note possibility of composite polar with variable geometry/flap: can exploit this to approximate the ideal polar across a range of design C_l, i.e. airspeed.

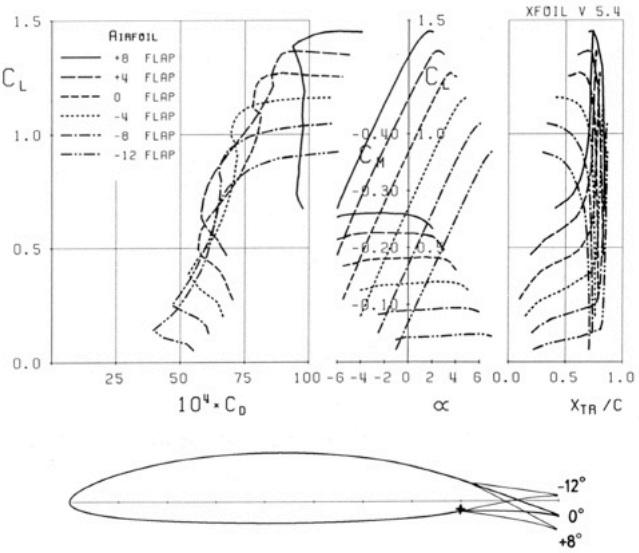

Fig. 1 Polars for laminar sailplane airfoil over range of flap settings [$Re = 10^6/\sqrt{(C_L)}$].

Drela

Airfoil nomenclature and performance — 6

1. Stall is dangerous as a considerable loss of altitude may be required for recovery, and control is lost.

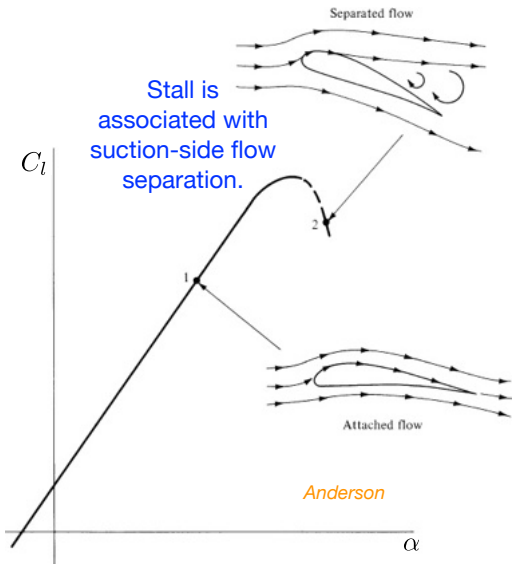

Anderson

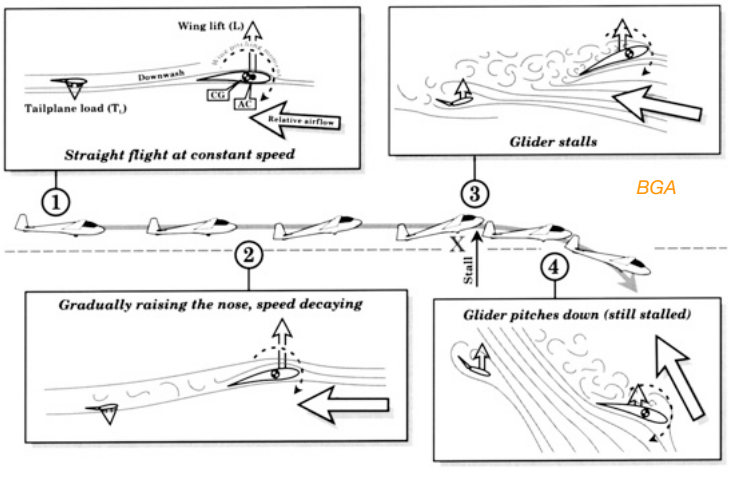

2. In addition there is the shape of the C_m-α curve to be considered. For stable stall recovery, it is desirable for the aircraft to tend to pitch nose-down i.e. for C_m to become more negative, post-stall. For an airfoil, this largely depends on the chordwise location where separation initiates.

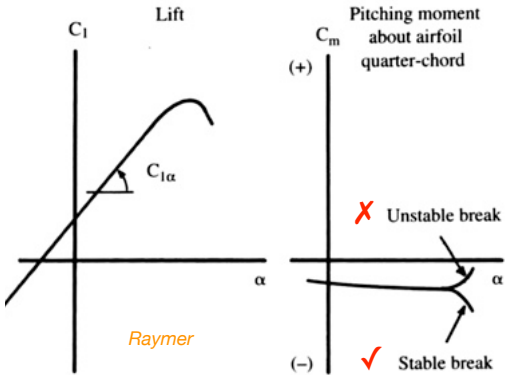

Raymer

23

High-lift systems

24

Airfoil $C_{l\max}$ and high-lift systems — 1

We start by examining $C_{l\max}$ for the basic/clean airfoil. The key determinants of $C_{l\max}$ are

1. Camber;
2. LE nose radius;
3. Maximum thickness/chord ratio, *t/c;*
4. Reynolds number (not geometry-related).

The higher $C_{l\max}$, the slower the aircraft will be able to fly:

$$V_{\min} = \sqrt{\frac{2}{\rho}\frac{W}{S}\frac{1}{C_{l\ \max}}}$$

A high basic value of $C_{l\max}$ may not be critically important if additional high-lift devices are employed.

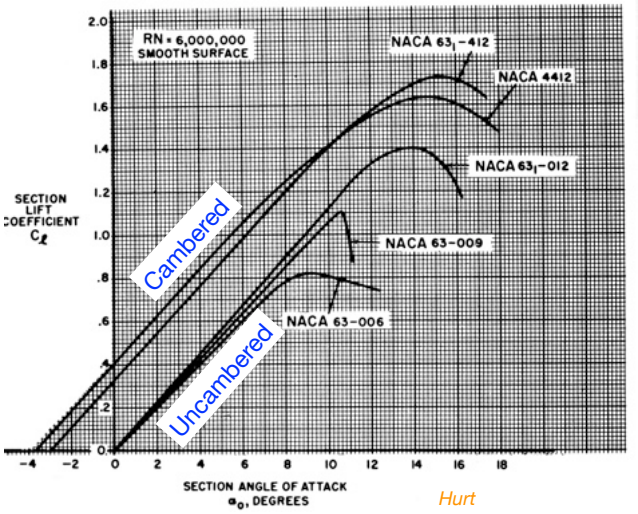

Hurt

1,2: Camber and nose radius.

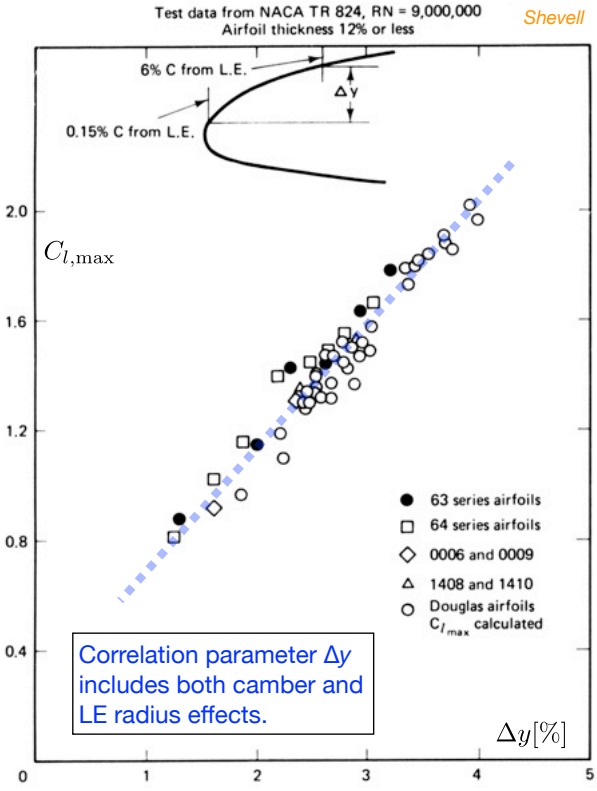

Shevell

Airfoil $C_{l\max}$ and high-lift systems — 2

Shevell

3,4: *t/c* ratio and *Re.*

Increasing thickness increases peak suction but also makes recovery pressure gradient increasingly adverse — there is a `happy medium'.

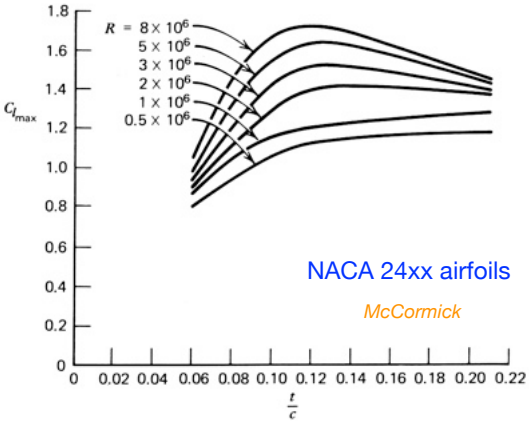

NACA 24xx airfoils

McCormick

Prediction of $C_{l\max}$ is difficult and generally, correlations of experimental data or (better) airfoil-specific experimental values are desirable.

ESDU (Engineering Sciences Data Unit) publish a number of correlations in this area. For plain airfoils, the relevant data item is ESDU 84026.

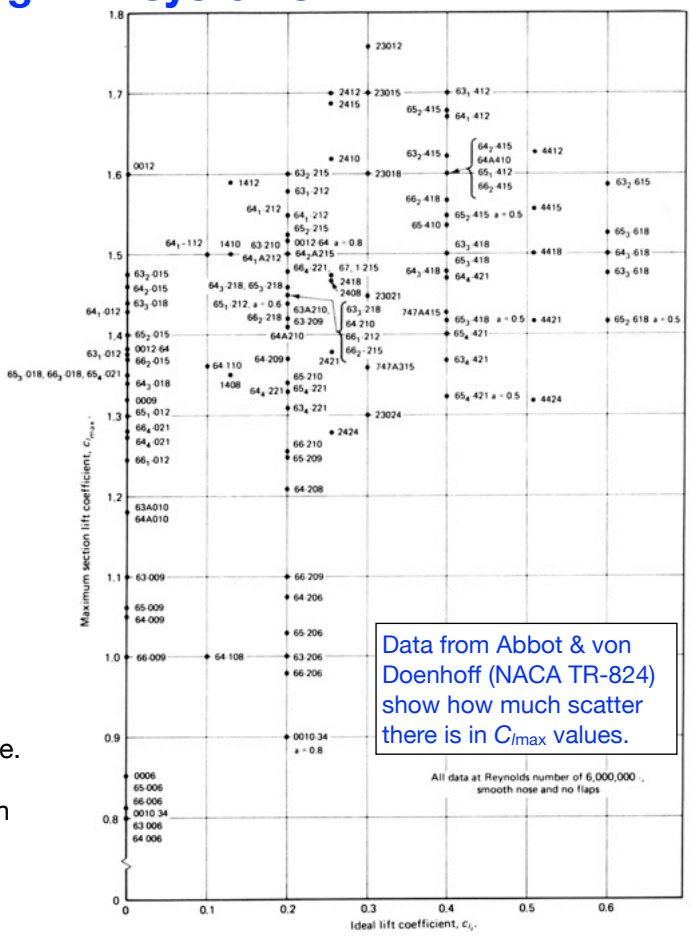

Data from Abbot & von Doenhoff (NACA TR-824) show how much scatter there is in $C_{l\max}$ values.

Airfoil $C_{l\max}$ and high-lift systems — 3

1. Now we consider geometry-changing devices, i.e. (TE) flaps and (LE) slats (sometimes a.k.a. LE flaps).
2. High-lift devices are now virtually standard equipment on all but the simplest/lightest aircraft.
3. The effect of deflecting a flap on airfoil performance is broadly similar to increasing camber *except* that the reference angle of attack (and wing area) is still defined w.r.t. the original chord line.
4. Note that the profile drag increases and the moment coefficient becomes more negative.

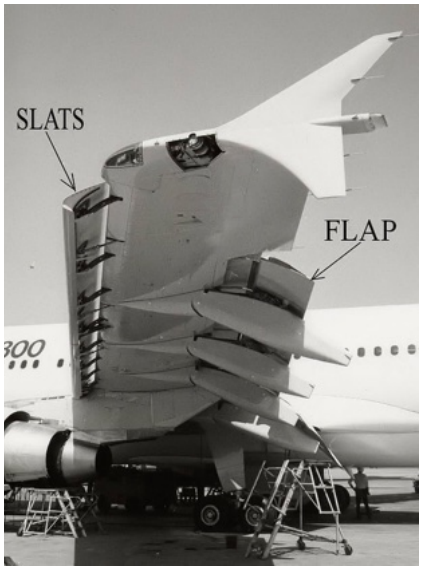

wikipedia

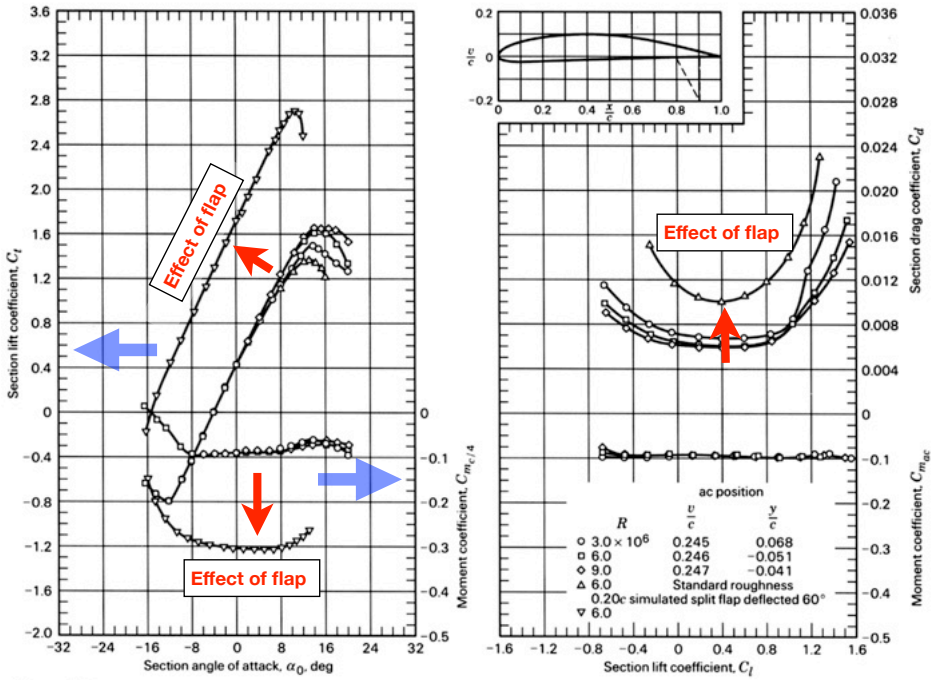

Figure 3.7 Aerodynamic characteristics of the NACA 4412 airfoil.

McCormick

Airfoil $C_{l\max}$ and high-lift systems — 4

5. Different flap + slat designs and their characteristics.

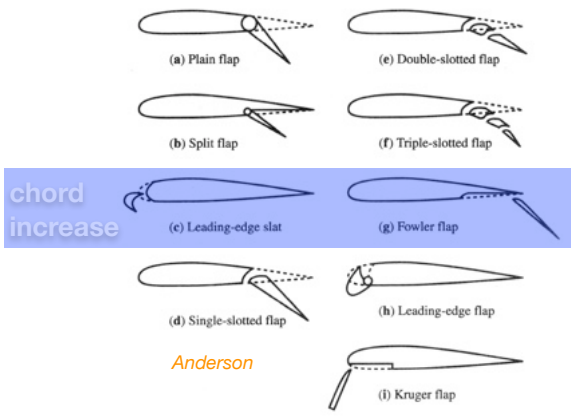

Anderson

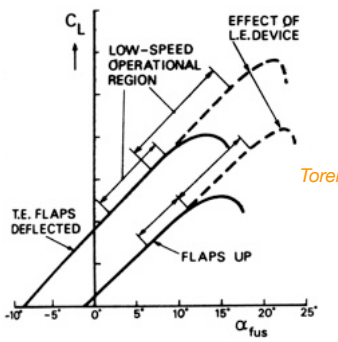

Torenbeek

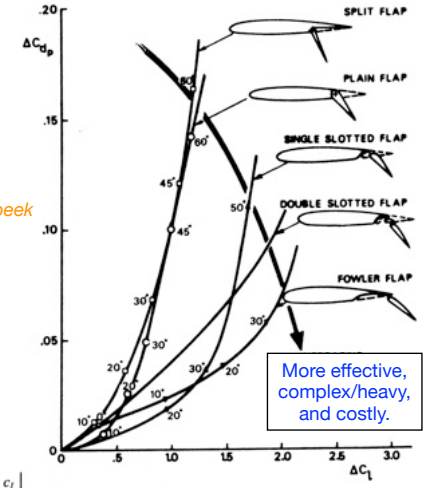

More effective, complex/heavy, and costly.

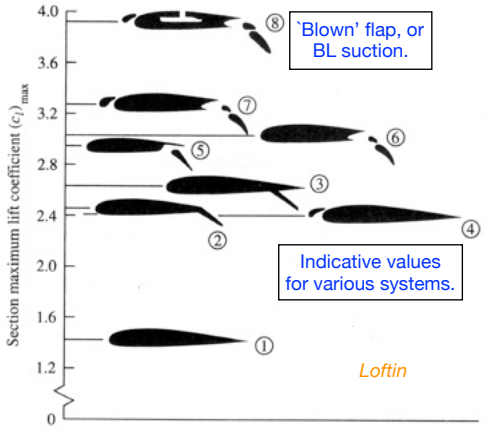

`Blown' flap, or BL suction.

Indicative values for various systems.

Loftin

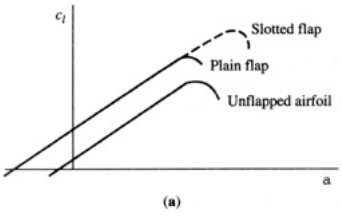

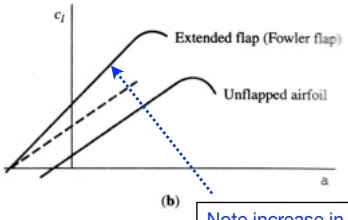

Note increase in lift curve slope owing to increased effective wing area.

Anderson

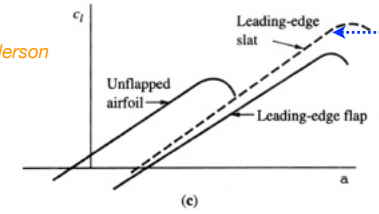

Airfoil $C_{l\max}$ and high-lift systems — 5

6. An 'incremental' contribution approach to estimating $C_{l\max}$ is generally used (so we also need the plain-airfoil value).

$$C_{l\,\max} = C_{l\,\max,\ \text{basic airfoil}} + \Delta C_{l\,\max,\ \text{LE}} + \Delta C_{l\,\max,\ \text{TE}}$$

Raymer

High-lift device	$\Delta C_{l_{max}}$
Flaps	
Plain and split	0.9
Slotted	1.3
Fowler	1.3 c′/c
Double slotted	1.6 c′/c
Triple slotted	1.9 c′/c
Leading-edge devices	
Fixed slot	0.2
Leading edge flap	0.3
Kruger flap	0.3
Slat	0.4 c′/c

Note the use of the extended chord ratio *c'/c.*

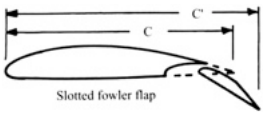

More extensive/detailed data correlations can be found in ESDU data items 94027, 94028, 94029, 94030, 94031.

7. The chordwise extents of high-lift devices are typically constrained by structural and fuel volume requirements.

Aircraft type	TE device chordwise extent	Maximum deflection (deg).
Personal/ utility	25-30%	35
Commuter, regional turboprop, business jet, jet transport	30-35%	45-50
Jet transport (slow landing/ short field/high W/S)	up to 40%	up to 50

Schaufele

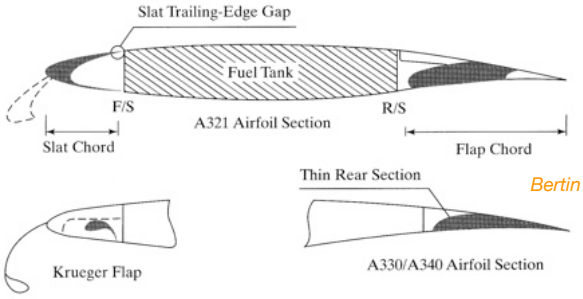

Bertin

Airfoil $C_{l\max}$ and high-lift systems — 6

8. The use of LE and TE devices to increase $C_{l\max}$ and also C_l/C_d during subsonic manoeuvres at high (less than maximum) C_l, but allowing good supersonic performance, is now standard practice for high-performance military/fighter aircraft.

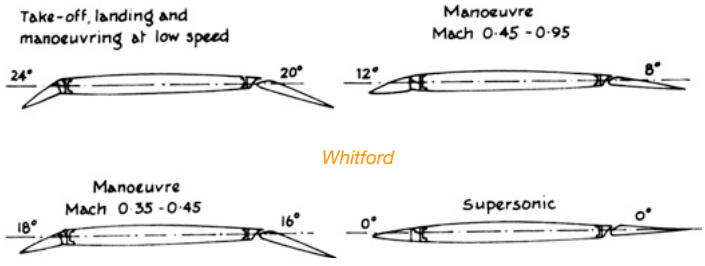

Whitford

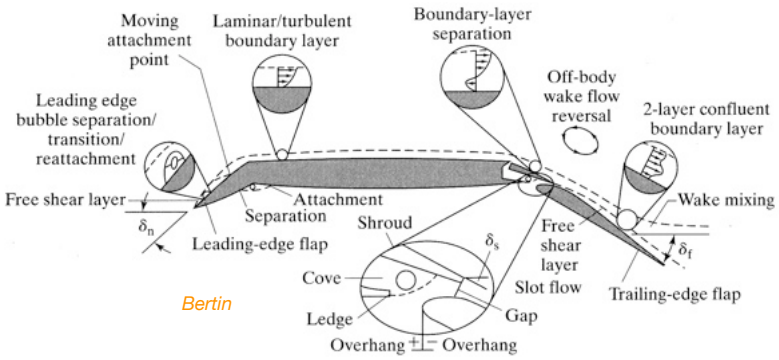

Bertin

Airliners.net

Effect of wing sweep — 1

1. Wing sweep is used on virtually all high-subsonic jet transport aircraft, which require high values of M_{DD} to maximize range parameter *ML/D*. For transonic flow, $\Lambda_{c/4}$ is taken as the relevant value.
2. The effect of sweep can be understood by considering that it is only the component of flow normal to the axis of the wing which produces substantial pressure changes (lift) and hence brings about critical Mach conditions. From geometry, $M_{CC} \approx M_{CC,\Lambda=0} / \cos\Lambda$.
3. However, there is a counter-effect: the value of *t/c* normal to the *c*/4 line is increased, which somewhat reduces the effectiveness of sweep to $M_{CC} \approx M_{CC,\Lambda=0} / \cos^m\Lambda$, where $m < 1$ is C_L-dependent.
4. Sweep also slightly increases the speed increment between M_{CC} and M_{DIV}. For M_{DIV} defined by $dC_D/dM=0.05$,

$$M_{DIV} \approx M_{CC}[1.02 + 0.08(1 - \cos\Lambda)]$$

5. The above discussion is for infinite-span swept wings but it works reasonably well for finite wings of $A>4$. For purposes of preliminary design, we now have enough information to estimate M_{DD} (M_{DIV}).

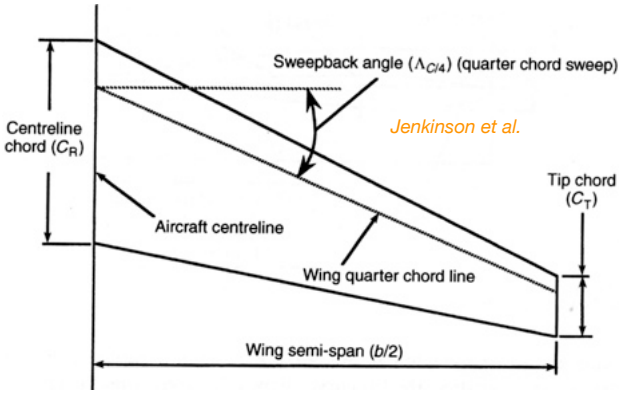

Jenkinson et al.

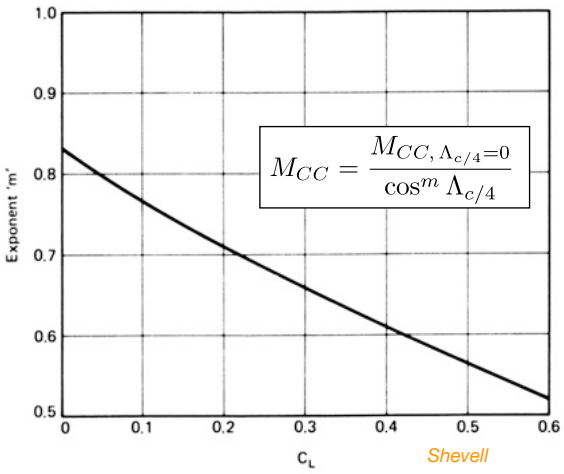

Shevell

Effect of wing sweep — 2

6. Given the revised estimate for M_{CC} with sweep, we can employ a further correlation to fit the incremental contribution of compressibility drag as a function of M. Note that there is a rise in drag even below M_{CC}, and that a 20-drag-count rise (ΔC_D=0.002) in drag occurs when $M/M_{CC}\simeq 1.025$ in the unswept case.
7. While sweep 'postpones the inevitable' by increasing Mach number for onset of compressibility effects, ultimately they still occur, and for M>1, a swept wing can have more drag than an unswept one, but a greater C_{Lmax}.

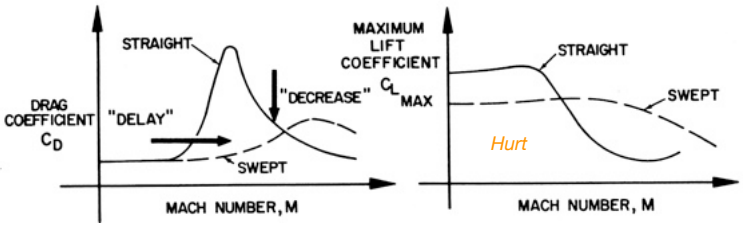

Shevell

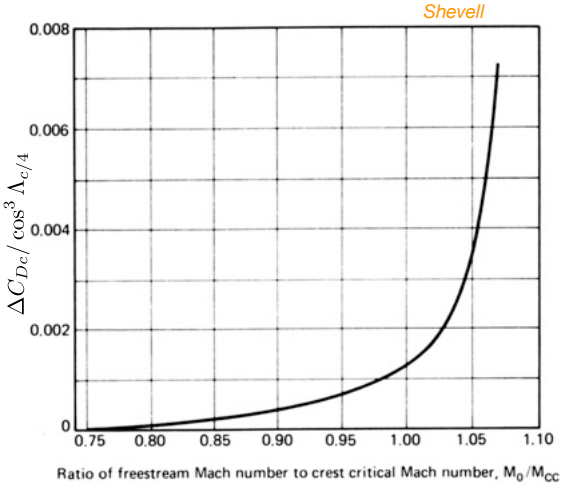

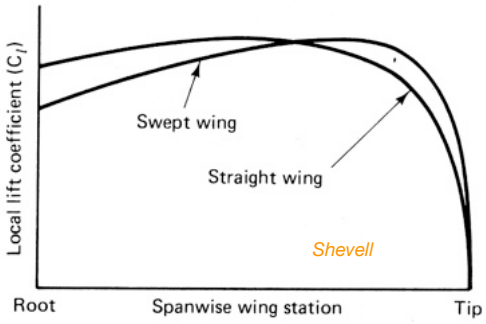

8. Sweep reduces the lift-curve slope, and changes the spanwise lift distribution in a way that reduces the span efficiency and promotes tip stall. To an extent, the latter effects can be compensated using wing twist/washout, but the best efficiency will then be tuned to a particular C_L value. Swept wings invariably have washout/twist.

Effect of wing sweep — 3

Indicative wing twist distribution for a jet transport.

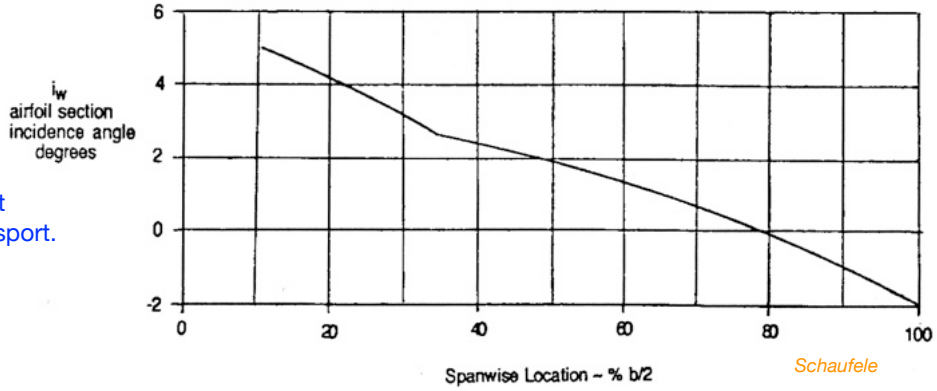

Schaufele

9. Sweep reduces the lift-curve slope and C_{Lmax}. Additionally, the effect of sweep on the spanwise lift distribution means that swept wings stall at lower C_{Lmax} values than unswept wings. An approximate derating from the maximum sectional value is:

$$C_{L_{\max}} = 0.9\, C_{l_{\max}} \cos\Lambda_{c/4}$$

10. Summary: to increase M_{DD},
    a. increase wing sweep
    b. decrease wing thickness ratio
    c. decrease aspect ratio/wing loading/C_L
    d. use a supercritical airfoil (alternatively, for the same M_{DD}, a supercritical airfoil will give a thicker/lighter wing).

Finite-wing high-lift devices — 1

$$C_{L\,\max} = C_{L\,\max,\,\text{basic wing}} + \Delta C_{L\,\max,\,\text{LE}} + \Delta C_{L\,\max,\,\text{TE}}$$
$$C_{L\,\max,\,\text{basic wing}} \approx 0.9 \cos \Lambda_{c/4} C_{l\,\max,\,\text{basic airfoil}}$$

1. We have already considered the effectiveness of high-lift devices in increasing airfoil $C_{l\max}$.
2. On finite wings, they usually cannot extend full-span owing to presence of ailerons, fuselage, engines.
3. Their effectiveness is diminished by 3D flows and sweep.
4. First, the incremental effectiveness of LE/TE devices is derated according to their relative 'flapped area'. Then we also allow for sweep and 3D flows. These considerations are combined in the approximation

$$\Delta C_{L_{\max}} = 0.9 \Delta C_{l_{\max}} \left(\frac{S_{\text{flapped}}}{S_{\text{ref}}} \right) \cos \Lambda_{\text{HL}}$$

Λ_{HL} is hinge-line sweep angle.

5. The incremental approach allows separate accounting for LE and TE devices, or multiple devices on each edge.
6. For take-off, devices are often deployed, but deflected less, to take account of desired high *L/D* as well as $C_{L\max}$. Typical take-off $\Delta C_{L\max}$ values are 60%—80% of the maxima.

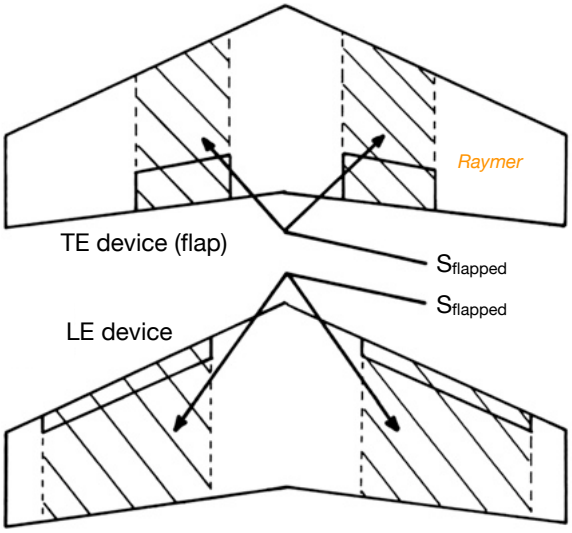

HIGH-LIFT DEVICE		TYPICAL FLAP ANGLE		$C_{L_{max}}/\cos\Lambda_{.25}$	
TRAILING EDGE	LEADING EDGE	TAKEOFF	LANDING	TAKEOFF	LANDING
PLAIN	-	20°	60°	1.40-1.60	1.70-2.00
SINGLE SLOTTED	-	20°	40°	1.50-1.70	1.80-2.20
FOWLER*	-	15°	40°	2.00-2.20	2.50-2.90
DOUBLE SLOTTED**	-	20°	50°	1.70-1.95	2.30-2.70
	SLAT			2.30-?.60	2.80-3.20
TRIPLE SLOTTED**	SLAT	20°	40°	2.40-2.70	3.20-3.50

Torenbeek

* SINGLE SLOTTED

** WITH VARYING AMOUNTS OF CHORD EXTENSION (FOWLER MOTION)

Finite-wing high-lift devices — 2

7. When accounting for spanwise extent of TE flaps, we have to make due allowance for roll control via ailerons unless their function is combined with flaps ('flaperons'), differential tail movement ('tailerons'), or spoilers, all of which require powered actuation. Typically, ailerons take up at least 30% of span.

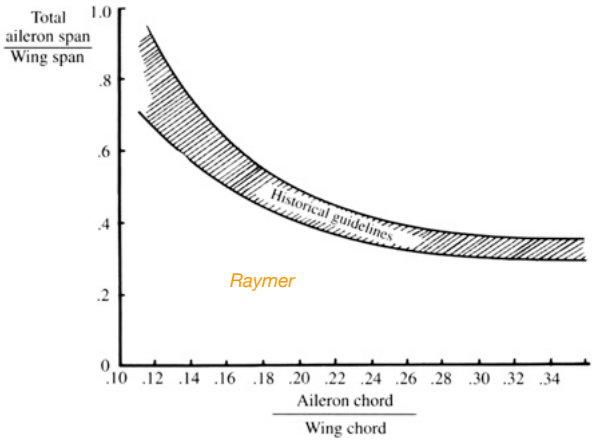

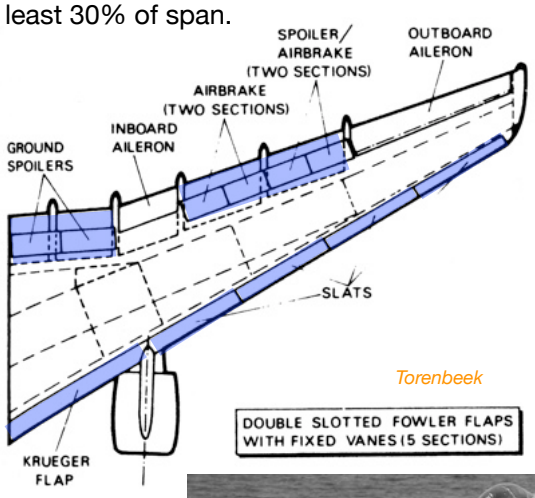

Hybrid combinations give more options, but may be costly, heavy.

F111 has tailerons and as much flap span as possible.

F18 uses flaperons but ailerons may be moved independently of flaps.

airliners.net

Examples of high-lift systems in use

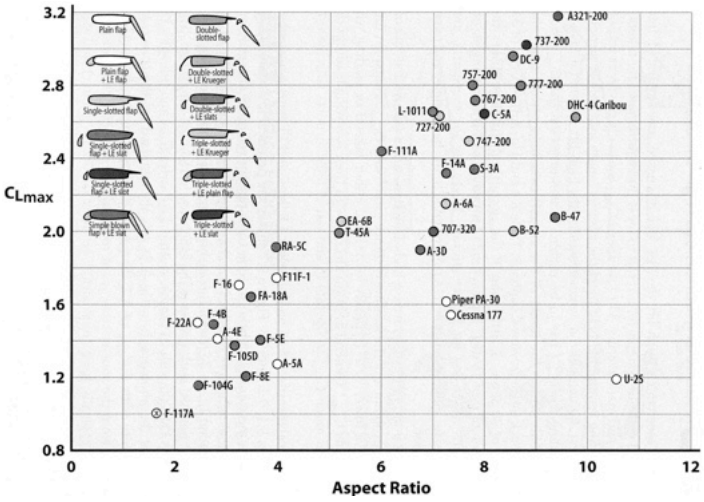

Nicolai & Carichner

Note: use of powered systems was confined to military types. 3 out of 4 were for carrier-capable aircraft.

Current Aircraft Mechanical High-Lift Systems

Aircraft	AR	$C_{l_{max}}$	Leading Edge	Trailing Edge
707-320	7.0	2.0	Full-span plain flap	Triple-slotted Fowler
E-6A	7.0	2.16	Improved 707-320 system	
727-200	7.1	2.62	1/3 Krueger, 2/3 span slats	Triple-slotted Fowler
737-200	8.83	3.05	Krueger IB, slats OB[a]	Triple-slotted Fowler
747-400	7.7	2.5	Krueger IB, slats OB	Triple-slotted Fowler
757-200	7.77	2.8	Full-span slats	Double-slotted Fowler
767-200	7.9	2.75	Full-span slats	Double slot IB, single slot OB
777-200	8.7	2.8	Full-span slats	Double slot IB, single slot OB
787	Var.	NA	Krueger IB, slats OB	Triple-slotted Fowler+variable camber
A321-200	9.5	3.2	Full span slats	Double slotted Fowler+drooped ailerons
L-1011	6.95	2.65	Full-span slats	Double-slotted Fowler
S-3A	7.8	2.36	Slats OB of engine	Single-slotted Fowler
DC-9	8.5	2.96	Ful-span slats	Full-span double-slotted flap
DHC-4	9.9	2.63	None	Full-span double-slotted flap
C-5A	8.0	2.64	Slots IB+slotted slats OB	Partial-span single-slotted Fowler
U-2S	10.6	1.21	None	Partial-span simple hinge flap
PA-30	7.3	1.6	None	Half-span plain flap
Cessna177	7.4	1.55	None	Half-span plain flap
B-47	9.42	2.05	Full-span slat	Partial-span Fowler
B-52G	8.56	2.0	None	Partial-span Fowler
F-16C	3.2	1.7	Full-span maneuver flap	Half-span plain flap
F-22A	2.36	1.48	Full-span maneuver flap	Full flaperon+drooped aileron
A-3D	6.75	1.9	Full-span slats	Partial-span single-slotted flap
F-4B	2.78	1.4	Full plain flap (blown)	Partial-span blown plain flap
A-4E	2.9	1.42	Automatic LE slats	1/2 split flap+drooped ailerons
RA-5C	4.0	1.9	Full-span plain flap	Partial-span plain flap (blown OB)
F-5E	3.7	1.4	Full-span plain flap	Partial-span single-slotted flap
A-6A	5.3	2.05	Full-span plain flaps	Partial-span Fowler flap
F-14A	7.25	2.35	Full-span LE slats	Full-span slotted flaps
F-111A	6.0	2.45	Full-span LE slats	Partial-span blown plain flap
F-117	1.65	0.95	None	None
F-18A	3.5	1.62	Full-span plain flap	Half-span single-slotted TE flap
F-105D	3.18	1.38	Full-span plain flap	Partial-span single-slotted flap
F-104G	2.45	1.12	Full-span plain flap	Blown flap+drooped aileron
T-45A	5.0	2.0	Full-span plain flap	2/3 span double-slotted flaps
F-8E	3.5	1.2	Full-span plain flap	2/3 plain flap+variable-incidence wing
F-11F	3.95	1.75	Full-span slats	Full-span plain flaps

[a]Abbreviations: IB, inboard; OB, outboard.

Compressibility effects

Compressibility effects on airfoil performance — 1

Recall that our treatment is mainly concerned with subsonic, up to onset transonic, freestream Mach numbers.

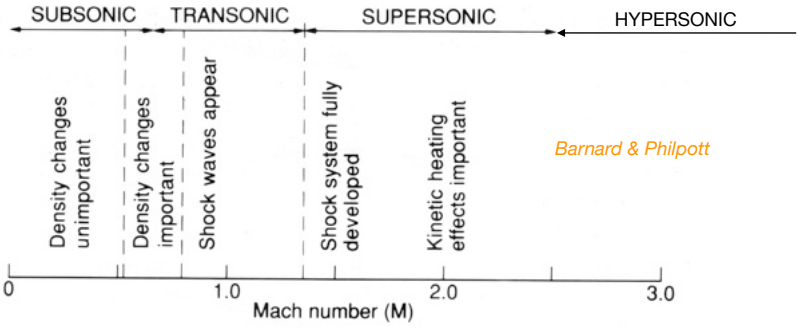

Barnard & Philpott

1. The general progression of airfoil shock structure with Mach number:

The critical freestream Mach number M_{cr} is the value for which the flow around the body (airfoil) first reaches M=1 locally.

Local supersonic flow and a compression shock arise at a 'critical' freestream M_∞<1.

For transonic flows, M_∞<1, the shock can produce flow separation and greatly increased drag.

Supersonic region grows to include entire upper and lower surfaces. Compression shock moves to TE.

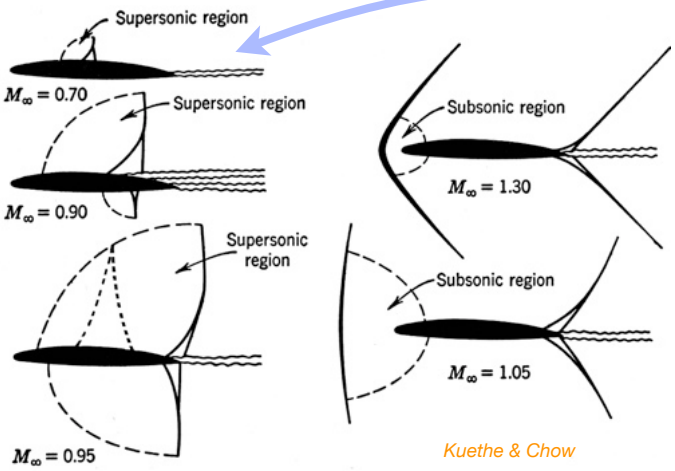

Generally, much less separation for supersonic flows but wave drag becomes dominant.

Bow shock appears at M_∞=1.

Kuethe & Chow

Compressibility effects on airfoil performance — 2

2. If we know the minimum airfoil pressure coefficient, C_{pmin} (corresponding to local fastest speed since C_p=1-(V_{local}/V_∞)^2) then we can use results from linearized compressible flow (either Prandtl-Glauert, P-G, or von Karman-Tsien corrections), and isentropic gas relations, to estimate M_{cr}.

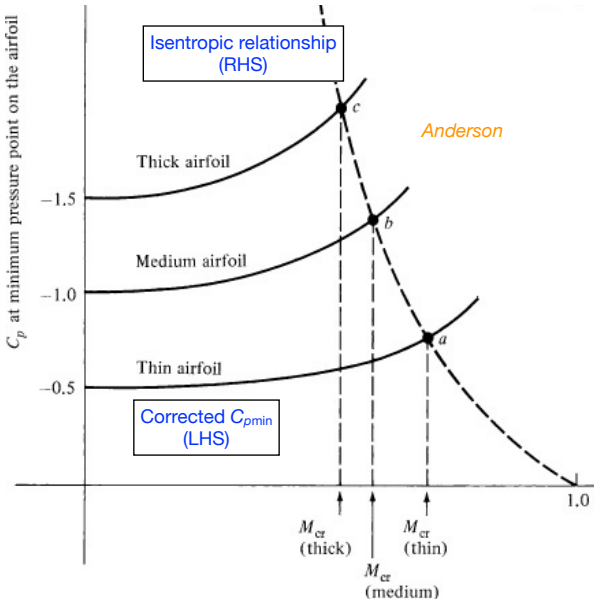

Anderson

For example, we set the P-G-corrected C_{pmin} equal to the relationship corresponding to an isentropic acceleration from a freestream condition (p_∞, M_∞) to M=1:

$$\frac{C_{p\,\min,0}}{\sqrt{1-M_\infty^2}} = \frac{2}{\gamma {M_\infty}^2}\left\{\left(\frac{1+[(\gamma-1)/2]{M_\infty}^2}{1+(\gamma-1)/2}\right)^{\gamma/(\gamma-1)} - 1\right\}$$

Solving this for M_∞ does give a good estimate of M_{cr}, but it is difficult to use in initial design, when, while we may be able to nominate C_l, it is difficult to know C_{pmin} (especially if we haven't even selected an airfoil).

3. Compressibility affects both lift and drag. As M=1 is approached, C_l initially increases (approximately according to the linearised P-G correction above: $C_l \approx C_{l0}/(1-M^2)^{0.5}$), but even more significantly, C_d starts to rise rapidly following M_{cr}. This is because the shock wave that terminates the locally supersonic region becomes strong enough to significantly thicken the BL and increase profile drag.

Compressibility effects on airfoil performance — 3

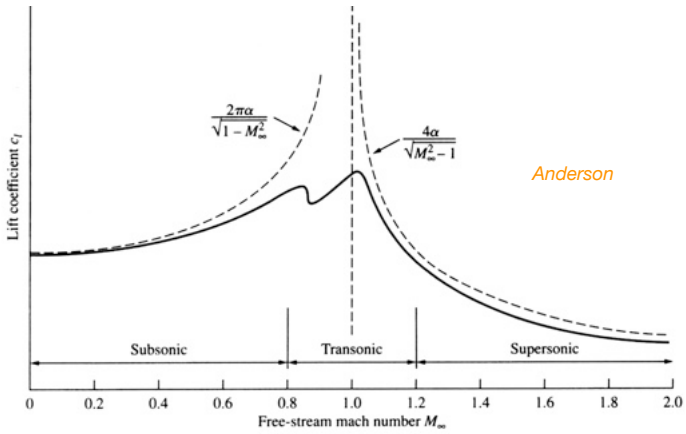

Figure 2.10 Sketch of a generic lift coefficient variation with Mach number.

4. Here are generic pictures of how C_l and C_d vary with Mach number. Linear theories do a reasonable job of estimating C_l vs M away from M=1, at least for attached flow. The task of estimating C_d is much more difficult since there (a) is no linear theory available in the subsonic regime and (b) the rise of C_d is associated with shock wave formation. Experiments and resulting data correlations are the basis for estimates in the transonic regime near M=1.

5. At Mach numbers just above M_{cr}, C_d is found to start rising steeply with M. The associated value, the drag divergence Mach number. M_{DD}, a.k.a. M_{DIV}, has various definitions, but is typically associated with a rise in C_d of a few percent, or say 20 *drag counts*, where 1cd=0.0001. M_{DD} is the basic design Mach number for efficient cruise of jet transport aircraft.

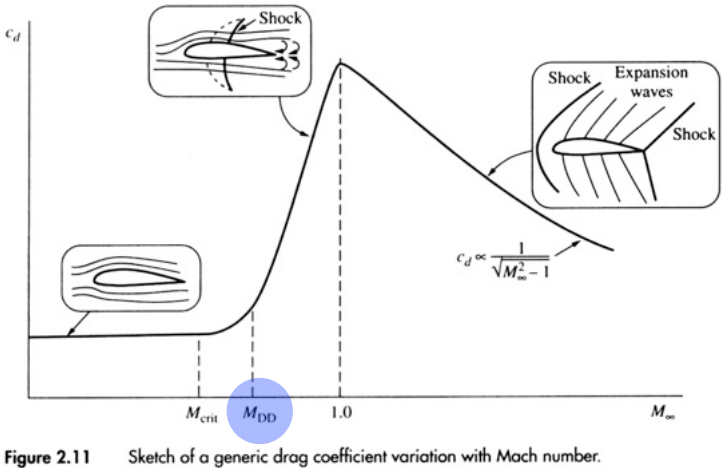

Figure 2.11 Sketch of a generic drag coefficient variation with Mach number.

Compressibility effects on airfoil performance — 4

6. M_{CR}, hence M_{DD}, will depend on primarily on airfoil thickness ratio t/c and C_l. We adopt Shevell's correlation approach, where the idea of the crest critical Mach number, M_{CC}, approximates M_{CR}. M_{DD}, a.k.a. M_{DIV}, typically is a few percent higher.
7. For now we'll leave the topic at estimation of M_{CC} for an unswept wing, and return to estimation of M_{DIV} when we consider wing sweep, Λ.
8. Shevell's correlations are for 'old-style' subsonic airfoils. For modern/supercritical airfoils, increase M_{CC} by 0.06.

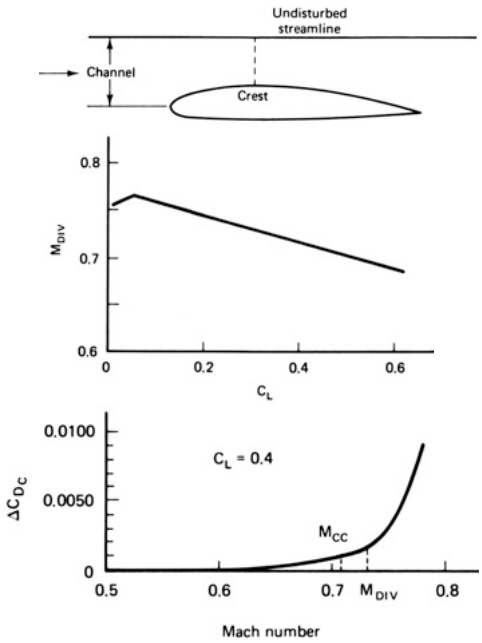

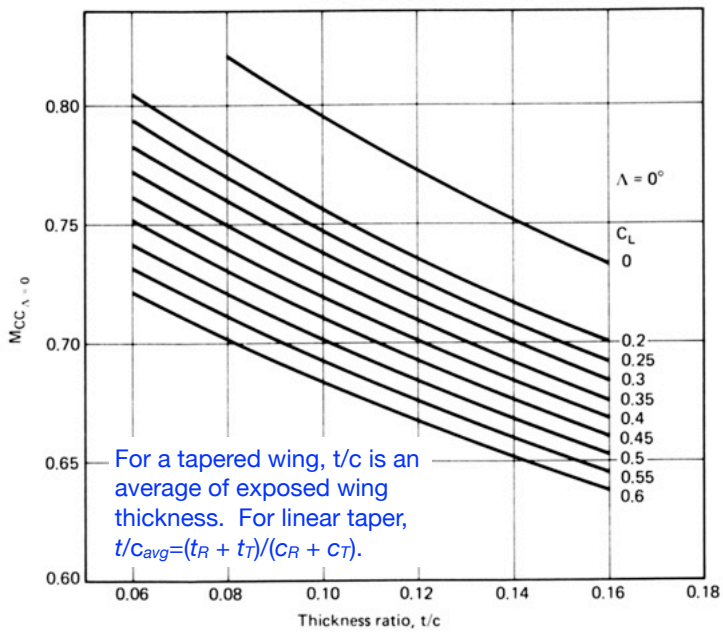

41

Wing planform

42

Finite-wing aerodynamics, whole-aircraft values

1. All real wings are finite/3D and this substantially affects their performance.
2. The convention we (and most others) take in design is to compute the wing reference area and geometry as though the fuselage were not present. (This can present to dilemmas if wing and body are extensively blended, or the wings are relatively small.) Interference factors allow for the fuselage effect.
3. The convention for coefficients of lift, drag etc is that upper-case subscripts (e.g. C_L) denote whole-aircraft/3D values, while those with lower-case subscripts (e.g. C_l) represent sectional/2D values. Forces are normalized by the dynamic pressure and the wing reference area S. Moments are further normalized with the MAC, and conventionally, moments are taken about the aircraft centre of gravity (CG) location.
4. Note the standard symbols given to key geometric values.

$$C_L = \frac{L}{\frac{1}{2}\rho V^2 S}$$
$$C_D = \frac{D}{\frac{1}{2}\rho V^2 S}$$
$$C_M = \frac{M}{\frac{1}{2}\rho V^2 S\,\bar{c}}$$

CG symbol

S	=	reference wing area
b	=	span
c	=	chord (distance LE to TE)
$\bar{c}$	=	mean aerodynamic chord, MAC
A	=	aspect ratio $= b^2/S$
λ	=	taper ratio $= c_{\text{tip}}/c_{\text{root}}$
Λ	=	sweep

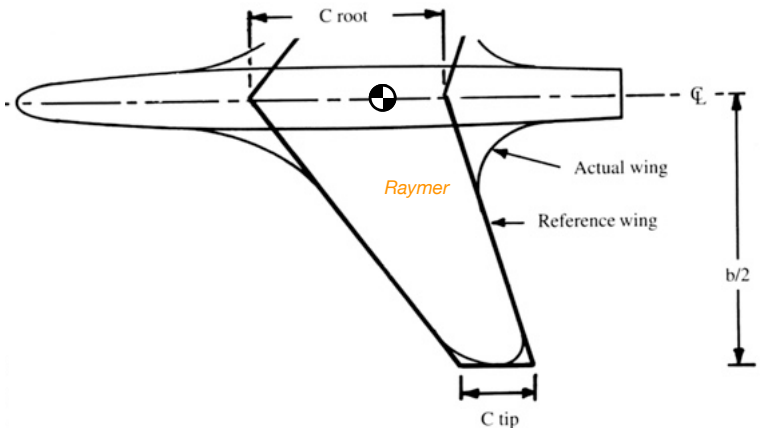

The (ESDU) idea of an equivalent trapezoidal planform

1. While wings can be of any shape and the optimal planforms are typically curved (e.g. elliptical), trapezoidal planforms (or some approximation to them) are most common in practice and it makes sense for initial considerations at least to deal with this shape.
2. The equivalent trapezoidal wing is typically obtained by projecting a fit through the actual wing planform to the aircraft centreline. It has the same exposed area as the actual wing exposed area, and the same tip chord and span. This is the ESDU definition.

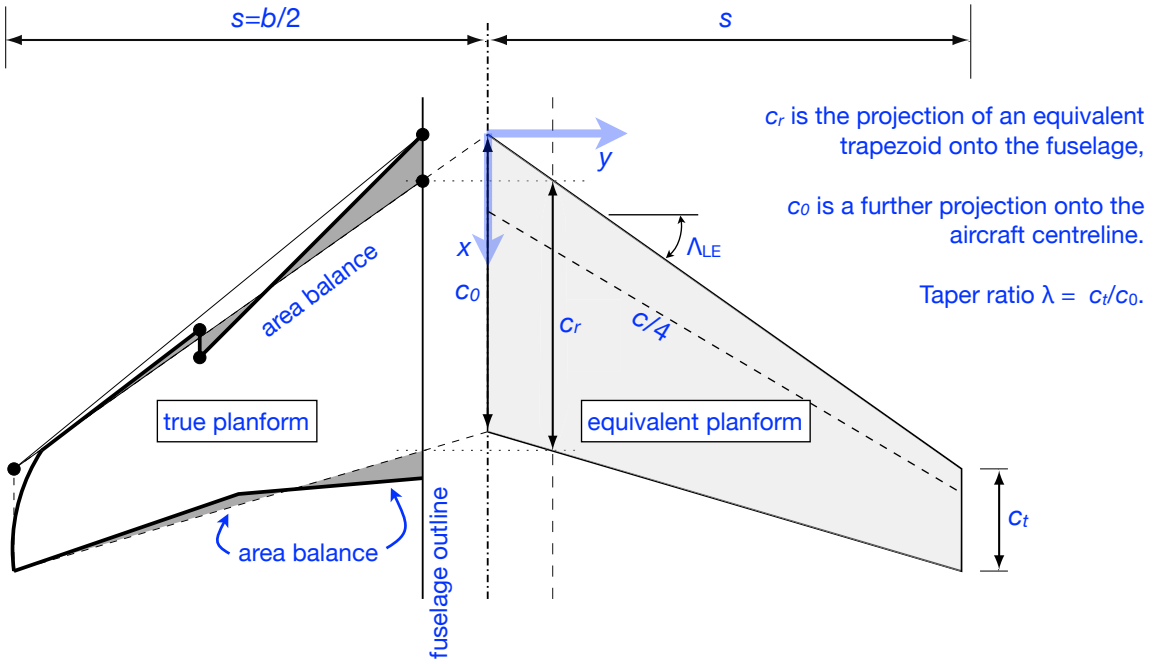

Two alternative wing reference area definitions FYI

Airbus

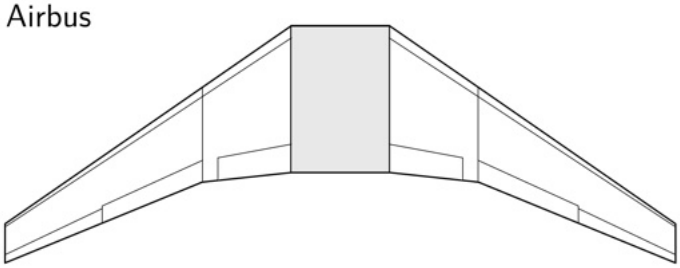

S = exposed wing area + area of rectangle inside fuselage between the leading and trailing edges at root

Wimpress (Boeing)

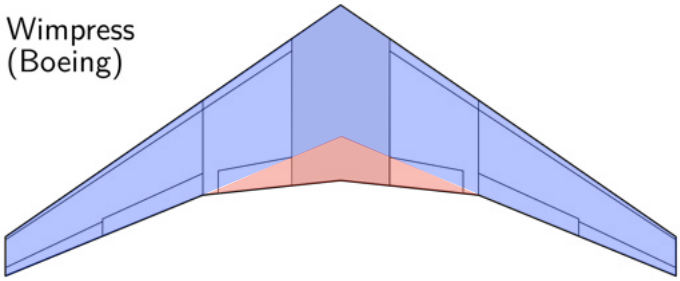

S = trapezoidal area + (exposed Yehudi area) + (covered Yehudi area) * fraction of exposed span at the break

It doesn't matter too much which definition one uses but the ESDU one is probably the simplest to use in initial design layout – i.e. base everything around a simple trapezoidal shape.

Yehudis (shape changes near wing root) are added to increase thickness and also to increase landing flap effectiveness.

Wing geometry — 2

1. Span $b = 2s$

2. Taper $\lambda = \dfrac{c_t}{c_0}$

3. Area $S = 2\displaystyle\int_0^{b/2} c(y)\,\mathrm{d}y = \frac{c_0 b}{2}(1+\lambda)$

NB: the formulae here involving λ are only applicable for cases where a trapezoidal planform approximation is appropriate.

4. Aspect ratio $A = \dfrac{b^2}{S} = \dfrac{b}{\bar{c}}$

5. Mean geometric chord $\bar{c}_{\mathrm{geom}} = \dfrac{1}{b/2}\displaystyle\int_0^{b/2} c(y)\,\mathrm{d}y = \frac{S}{b} = \frac{c_0}{2}(1+\lambda)$

6. Mean aerodynamic chord $\bar{c} = \dfrac{2}{S}\displaystyle\int_0^{b/2} c^2(y)\,\mathrm{d}y = \frac{2c_0}{3}\frac{1+\lambda+\lambda^2}{1+\lambda}$

NB: MAC is the key chord value.

7. Sweep $\Lambda,\ \Lambda_{c/4},\ \Lambda_{\mathrm{LE}}, \Lambda_{\mathrm{TE}}$

8. Geometric twist (washout)

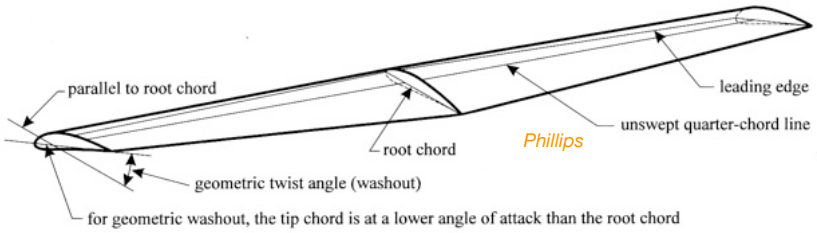

8. Dihedral angle

Aerodynamic centre of a lifting surface

As for an airfoil, the *aerodynamic centre* (or a.c.) of a wing is the moment reference point for which the pitching moment coefficient C_M is independent of the angle of attack.

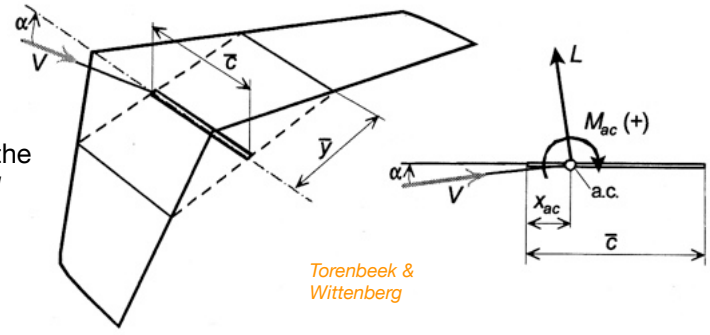

If the airfoil section is the same along the span and the wing is untwisted then the *mean aerodynamic chord* (MAC) and its spanwise location are given by the integral expressions

$$\bar{c} = \frac{2}{S}\int_0^{b/2} c^2\,\mathrm{d}y \qquad \bar{y} = \frac{2}{S}\int_0^{b/2} c\,y\,\mathrm{d}y$$

For a simple trapezoidal wing shape, these integrals provide

$$\frac{\bar{c}}{c_r} = \frac{2(1+\lambda+\lambda^2)}{3(1+\lambda)} \qquad \frac{\bar{y}}{b/2} = \frac{1+2\lambda}{3(1+\lambda)} \qquad \text{and} \qquad \frac{x_{LE_{\mathrm{MAC}}}}{c_r} = \left(\frac{1+2\lambda}{12}\right) A \tan\Lambda_{LE}$$

where the taper ratio $\lambda = \dfrac{c_t}{c_r}$

Those values as well as the longitudinal location of the MAC can be found for a trapezoidal wing shape using a simple geometric construction:

The longitudinal location of the aerodynamic centre on the wing, x_{ac}, is typically close to $\bar{c}/4$.

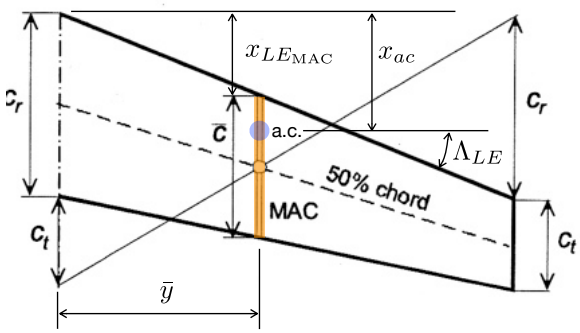

For more complicated planforms, look for calculation methods online, for example at:

http://www.dept.aoe.vt.edu/~mason/Mason_f/MRsoft.html

Wing geometry — 3

The mean aerodynamic chord (MAC) and its streamwise location are centrally important in determination of aircraft longitudinal balance and stability.

$$\bar{c} = \frac{2}{S}\int_0^{b/2} c^2(y)\,\mathrm{d}y = \frac{2c_0}{3}\frac{1+\lambda+\lambda^2}{1+\lambda}$$

MAC is the centroidal chord.

If the wing planform can be reasonably approximated by a trapezoid, then the MAC and its spanwise and streamwise locations can be determined using a simple graphical procedure shown below.

If the wing planform is more complicated then one should use the analytical definition. For a wing that is an assembly of trapezoidal shapes, ESDU 76003 supplies formulae that can be used, but typically the integrals are simple enough to evaluate.

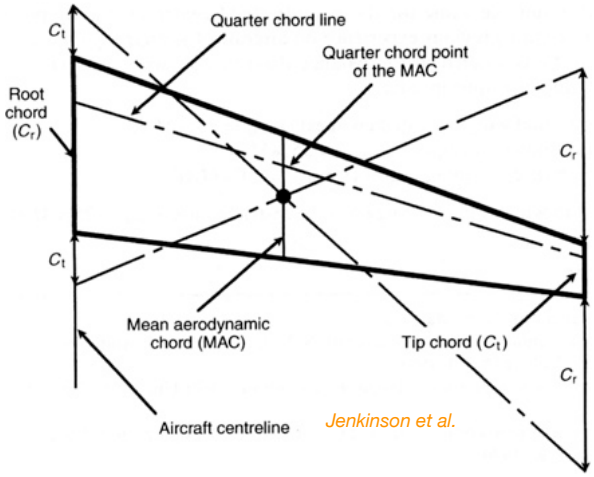

Jenkinson et al.

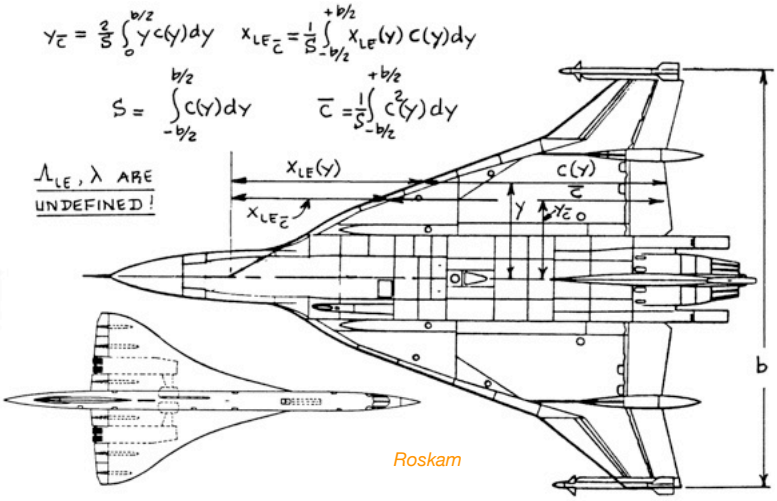

Roskam

Figure 2.7 Reference Geometry for Arbitrary Wings

Finite-wing effects on lift and drag — aspect ratio *A*

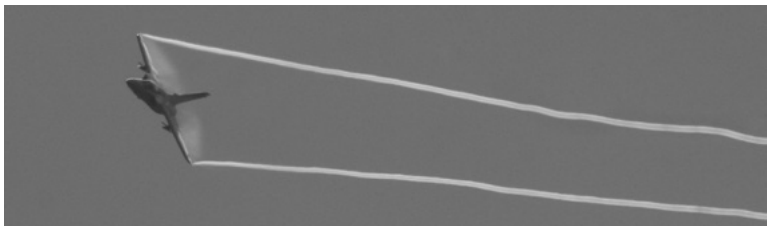

Vortices that trail from wingtips alter the flow about the remainder of the wing as well, by inducing downwash. This reduces the effective angle of attack, especially near the tips. Even in the inviscid case, the lift vector is inclined reward by this, resulting in a lift-induced drag.

Induced drag can be estimated via linear/inviscid calculations.

These tip effects decrease as the wing aspect ratio (span/average chord) increases (i.e. as the wing tips get further apart), or if the amount of lift required decreases.

Two main results when considering the lift and drag of the whole wing:

1. The whole-wing lift curve slope $\partial C_L/\partial\alpha$ reduces from the airfoil (i.e. infinite wing) value.
2. The whole-wing C_D increases by an amount (called induced drag, C_{Di}) proportional to C_L^2, and inversely proportional to aspect ratio A.

$$C_{D\,i} = C_L^2/\pi A u, \quad u \le 1$$

u is called span efficiency

Both these effects can be well accounted for theoretically at all but very small aspect ratios:

Experiments at various wing aspect ratios *A*.

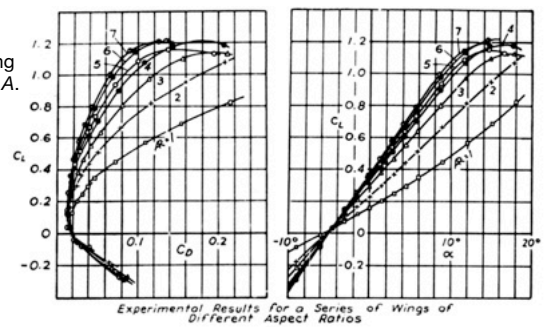

Experimental Results for a Series of Wings of Different Aspect Ratios

Corrected to a common aspect ratio *A*=5.

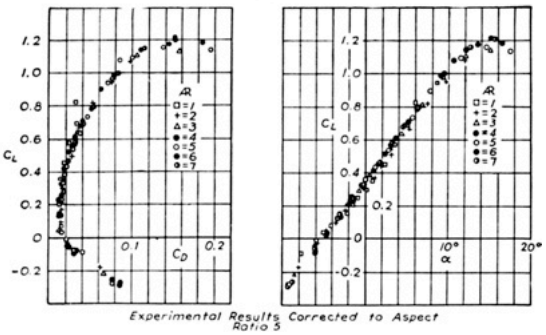

Prandtl

Experimental Results Corrected to Aspect Ratio 5

Finite-wing effects on lift and drag — wing planform - 1

It can be shown that an elliptical wing planform is the most efficient (for incompressible flow at least) — for this shape the induced angle of downwash produced by trailing vortices is equal all the way along the span. Any other shape has reduced efficiency (i.e. more induced drag).

$$C_{Di} = \frac{C_L^2}{\pi A u} \equiv \frac{C_L^2}{\pi A}(1+\delta)$$

where u=1, δ=0 for an elliptical planform. Larger δ (i.e. smaller span efficiency u) increases drag/reduces efficiency.

δ can be calculated for any planform, and a common one is an unswept wing with linear taper ratio λ (see plot).

Note that twisting the wing, e.g. adding washout, can change δ (perhaps favourably) — these calculations are for untwisted wings, but twist is often required for improved handling qualities.

δ is less than 0.02 (u>0.98) for λ ≈ 0.35, aspect ratio A < 10.

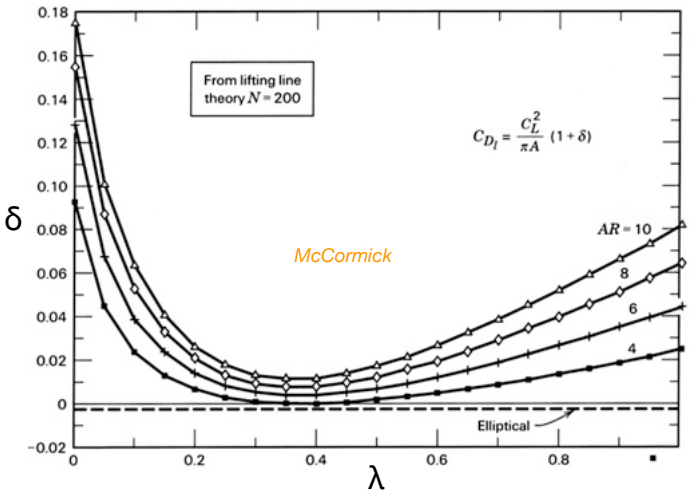

Finite-wing effects on lift and drag — wing planform - 2

Shown below are three wing planforms without twist, along with their computed circulation distributions at some non-zero lift. The elliptic component of the circulation $2bV_\infty A_1 \sin\theta$ is shown as a dotted line.

Even the crude constant-chord wing is 96% efficient (at A = 10), while a double-tapered wing is clearly almost as good as a fully elliptic planform. Three-panel wings (see bottom) are the practical ultimate.

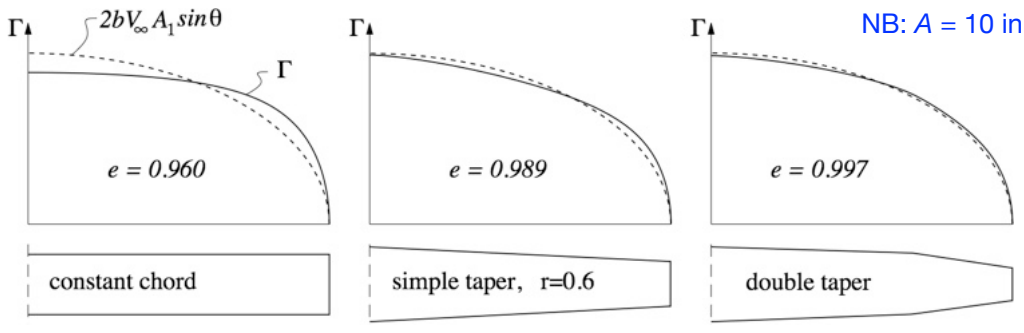

NB: A = 10 in each case.

Note however that the value of e (u) depends on the aspect ratio: somewhat surprisingly, as A increases, a rectangular wing gets progressively *less* efficient than an elliptical one.

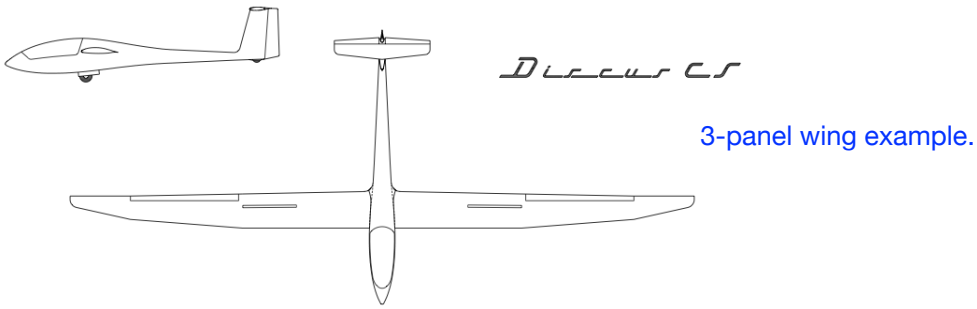

3-panel wing example.

Wing layout parameters

1. Reference wing planform = equivalent trapezoid is enough to start with, modify if necessary; reference area (S) will be determined in constraint analysis stages.
2. Aspect ratio: increasing aspect ratio (seems like a good idea… at first!):
   a. Reduces induced drag (increases subsonic L/D max) 🙂
   b. Increases stall AOA 🙂 (but very low aspect ratios have less abrupt stalling behaviour)
   c. Increases lift curve slope 🙂
   d. Increases wing weight 😕 😕
3. Taper ratio: a moderate reduces induced drag 🙂, too much promotes tip stall problems 😕
4. Sweep: use ‘just enough’ to overcome compressibility effects 🙂, since wing sweep also
   a. Decreases lift curve slope 😕
   b. Reduces effectiveness of high-lift systems 😕
   c. Exacerbates tip-stall and handling problems 😕
   d. Increases wing weight 😕
5. Airfoil choice as appropriate for type, generally as thick as can be tolerated. More thickness:
   a. Reduces M_{DD} 😕
   b. Increases $C_{L\max}$ (up to a point) 🙂
   c. Reduces wing weight (spar caps can be smaller for equivalent bending strength) 🙂
   d. Adds stowage volume for wing fuel and undercarriage 🙂
6. Twist, incidence, dihedral…